PAPER

Compactly supported Wannier functions and strictly local projectors

IOP Publishing Journal of Physics A: Mathematical and Theoretical
J. Phys. A: Math. Theor. **54** (2021) 335302 (39pp) https://doi.org/10.1088/1751-8121/ac1167

Compactly supported Wannier functions and strictly local projectors

Pratik Sathe, Fenner Harper and Rahul Roy*

Mani L Bhaumik Institute for Theoretical Physics, Department of Physics and Astronomy, University of California at Los Angeles, Los Angeles, CA 90095, United States of America

E-mail: psathe@physics.ucla.edu and rroy@physics.ucla.edu

Received 13 August 2020, revised 28 June 2021
Accepted for publication 6 July 2021
Published 28 July 2021

Abstract

Wannier functions that are maximally localized help in understanding many properties of crystalline materials. In the absence of topological obstructions, they are at least exponentially localized. In some cases such as flat-band Hamiltonians, it is possible to construct Wannier functions that are even more localized, so that they are compactly supported thus having zero support outside their corresponding locations. Under what general conditions is it possible to construct compactly supported Wannier functions? We answer this question in this paper. Specifically, we show that in $1d$ non-interacting tight-binding models, strict locality of the projection operator is a necessary and sufficient condition for a subspace to be spanned by a compactly supported orthogonal basis, independent of lattice translation symmetry. For any strictly local projector, we provide a procedure for obtaining such a basis. For higher dimensional systems, we discuss some additional conditions under which an occupied subspace is spanned by a compactly supported orthogonal basis, and show that the corresponding projectors are topologically trivial in many cases. We also show that a projector in arbitrary dimensions is strictly local if and only if for any chosen axis, its image is spanned by hybrid Wannier functions that are compactly supported along that axis.

Keywords: Wannier functions, localization, tight-binding models, band projectors, strict localization, compactly supported wavefunctions

(Some figures may appear in colour only in the online journal)

*Author to whom any correspondence should be addressed.

1. Introduction

Extended Bloch wavefunctions and localized Wannier functions (WFs) [1] are two common choices of basis vectors for a Bloch band. Localized WFs have applications in a number of fields, including the modern theory of polarization [2], orbital magnetization [3], quantum transport [4] and tight binding interpolation [5, 6]. Consequently, conditions required for the existence of localized WFs have been investigated extensively. Isolated bands of $1d$ inversion symmetric systems are always spanned by exponentially localized WFs as shown by Kohn [7]. The localization properties of WFs can often be inferred from the localization properties of the associated band projector. For instance, band projectors often possess real space matrix elements which decay exponentially [8], leading to generalizations [9, 10] of Kohn's result.

Because of the importance of obtaining localized WFs, there has been significant interest in obtaining WFs that are as localized as possible. A popular variational approach seeks localized WFs by numerically minimizing the second moment of the WFs around their centers [11]. It has been shown that maximally localized WFs decay exponentially (or faster) in $1d$ systems, with extensions proved for higher dimensional systems in the absence of topological obstructions [12].

A related, and sometimes more extreme form of wavefunction localization is compact support or strict localization in lattice models, wherein a wavefunction has non-zero support only over a finite set of orbitals of the lattice. Wavefunctions that are linear combinations of a finite set of orbitals bear a close analogy to Boys orbitals [13] which are studied in chemistry in the context of chemical bonding and other applications. The wavefunctions of Bloch electrons deep under the Fermi level are also expected to correspond to compactly supported (CS) WFs. Additionally, in some applications, it is useful to approximate highly localized WFs by CS wavefunctions [14–17].

Non-orthogonal bases consisting of CS wavefunctions, also known as CS Wannier-type functions have also received significant attention [18–20]. CS Wannier-type functions exist most commonly in strictly local (SL) flat-band Hamiltonians [21] in the context of which they are also known as compact localized states (CLSs). Such bases help in understanding a number of many-body quantum phenomena (see [22] for a review), including novel superconducting phases in multi-layer twisted graphene [23, 24]. CLSs have been used to classify and construct flat-band Hamiltonians [25–27]. Models so constructed are often made interacting, in order to study interesting many-body quantum phenomena arising in such contexts. For example, orthogonal CLSs have been used to construct models with many-body localized states [28] and quantum scar states [29] in flat-band systems. Orthogonal CLSs that span an entire flat band are precisely CS WFs of the flat band. Indeed, the conditions associated with the existence of orthogonal CLSs spanning flat bands and of CS WFs in systems without flat bands are closely related.

Yet another variant of WFs are hybrid WFs [30], that are localized and Wannier-like along one direction, and Bloch wave-like along the other directions. Localized hybrid WFs have a number of applications, including the study of twisted bilayer graphene [31], and characterization of static [32–34] and Floquet topological insulators [35]. Similar to CS WFs, a set of hybrid WFs that are CS along one of the axes can span a band in some cases. We refer to such functions as CS hybrid WFs.

While conditions associated with the existence of exponentially localized WFs, and of CLSs have been studied, those required for the existence of CS WFs and CS hybrid WFs remain unexplored. These considerations motivate us to pose the following questions: in a tight-binding lattice model, given an arbitrary set of occupied states, is there a way of determining whether their span possesses a CS Wannier basis? Analogously, in the absence of lattice translational

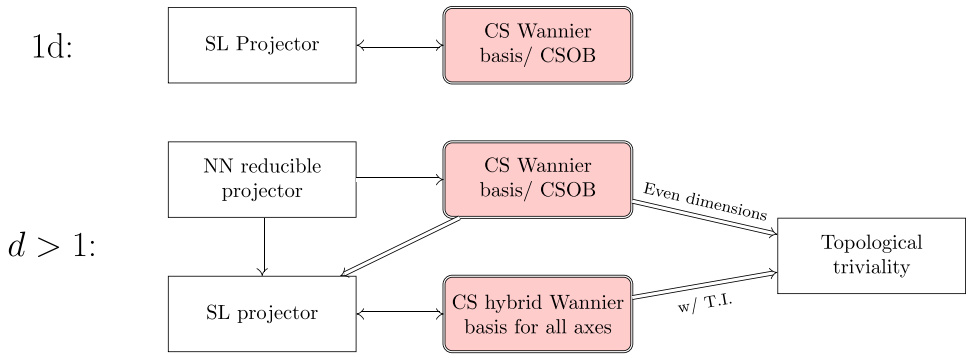

Figure 1. Summary of the main results of this paper. All the statements hold true independent of whether the system is translationally invariant (TI), except for the statement connecting the existence of CS hybrid Wannier basis for all axes to topological triviality.

invariance, under what conditions can the occupied subspace be spanned by an orthogonal basis of CS wavefunctions? We call such a basis a CS orthogonal basis or a CSOB in short. We show that the localization properties of the associated projector has a direct bearing on these questions. For 1d systems, we answer this question completely, showing an equivalence between strict locality of an orthogonal basis and strict locality of the associated orthogonal projector. For higher dimensional systems, we obtain necessary and sufficient conditions for the existence of such a basis, as well as for CS hybrid WFs. Our main results are summarized below.

Main result. For an arbitrary subspace spanned by single particle states in a non-interacting tight-binding model, independent of translational invariance, the following statements are true.

(a) In 1d systems, an orthogonal basis consisting of CS wavefunctions (i.e. a CSOB) spanning the subspace exists if and only if the associated orthogonal projector is SL.
(b) For a lattice in d dimensions, CS hybrid WFs localized along an axis exist for any choice (out of d possible choices) of the localization axis if and only if the associated band projector is SL.
(c) For arbitrary dimensional lattices, if the space is spanned by a CSOB, then the projector onto it is SL. If a projector is of a nearest neighbor (NN) form (or reducible to this form via a change of primitive vectors, or unit cell enlargement), its span possesses a CSOB.

Localization properties of WFs are closely related to the associated bands' topology [36–39]. Indeed, for many classes of Hamiltonians, exponentially localized WFs exist if and only if the band is topologically trivial. Hence, in addition to the main result, we also discuss topological properties of projectors associated with CSOBs and CS hybrid WFs. In particular, using existing results from the literature, we show that all TI SL projectors in $d > 1$ are topologically trivial. Moreover, for even dimensional systems, we show that if a space is spanned by a CSOB, then it is necessarily Chern trivial, irrespective of translational invariance. We also show that if CS hybrid WFs exist for any choice of the localization axis, the corresponding projector is *necessarily* topologically trivial for a TI system. This contrasts with exponentially localized hybrid WFs, which can be constructed for any band regardless of its topological properties [11, 40]. We summarize the main results as well as these extra results in figure 1.

We note that each of the three parts of the main result consists of a necessary condition and a sufficient condition for the existence of a CSOB (or a CS hybrid WFs). The necessary

condition in all cases is that the projector should be SL, and is straightforward to prove. Proving the sufficient condition is harder, and hence a significant portion of this paper deals with this aspect. Since the sufficient conditions are different for $1d$ and higher dimensions, these two cases are discussed separately. In section 2, we discuss the notation and definitions used in this paper, and prove the necessary direction from the main result. In addition, we also discuss the relationship between CLSs and CS Wanner-type functions, and show how to obtain non-orthogonal CLSs corresponding to any SL projector. In section 3, we prove by construction for $1d$ systems, that the image of any SL projector is spanned by a CSOB (or a CS Wannier basis if TI). Similarly, in section 4, we prove the sufficient part of points (b) and (c) of the main result. In addition we prove the extra results pertaining to topological triviality mentioned above. We conclude the paper with section 5, and provide a simple method for constructing some SL projectors in appendix A.2.

2. Preliminary discussion

In this section, we discuss some basic definitions and notation used in this paper as well as the connections between CLSs that arise in flat-band systems, and CS Wannier-functions associated with SL projectors. We also prove the sufficient part of the main result.

2.1. Notation

We consider d dimensional tight-binding models, with any (single particle) operator being represented by a matrix with rows and columns labeled by pairs of indices $(\vec{r}, i)$, with $\vec{r} \in \mathbb{Z}^d$ denoting a Bravais lattice site position, and $i \in \{1, \ldots, n_{\vec{r}}\}$ denoting the orbital index (which subsumes all quantum numbers, including spin quantum numbers if present). Our conclusions remain valid for finite lattices as well, for which we replace $\mathbb{Z}^d$ by an appropriate set of integer tuples. We denote a position basis vector by $|\vec{r}, i\rangle$, and refer to it as orbital i at site $\vec{r}$.

Henceforth, we use the terms site and cell interchangeably. Specifically, a cell at location $\vec{r}$ will mean the same as the site at location $\vec{r}$. By a supercell representation of the lattice, we mean a labeling scheme in which multiple sites in the original lattice representation are grouped together to form a new site. This reversible transformation involves relabeling of quantum numbers, as described in section 3.3.

We denote the Hilbert space associated with all the orbitals at cell $\vec{r}$ by $\mathcal{H}^{\vec{r}}$, and the total Hilbert space by $\mathcal{H}_{\text{total}}$. We note that

$$\mathcal{H}_{\text{total}} = \bigoplus_{\vec{r} \in \mathbb{Z}^d} \mathcal{H}^{\vec{r}}, \tag{1}$$

with $\oplus$ denoting a direct sum. In general, the number of orbitals at cell $\vec{r}$, denoted by $n_{\vec{r}}$, may be different for different cells, and our conclusions do not depend on them being equal. For notational simplicity, we assume without loss of generality that $n_{\vec{r}} = n$ is independent of the location. For systems with translational invariance, this condition is automatically satisfied. Additionally we find it convenient to rewrite $\mathcal{H}_{\text{total}}$ as,

$$\mathcal{H}_{\text{total}} = \mathbb{Z}^{\otimes d} \otimes \mathcal{H}, \tag{2}$$

where $\mathcal{H}$ denotes the n-dimensional orbital space. We refer to any orthonormal basis vectors of $\mathcal{H}$ as orbitals.

In this paper, we consider orthogonal projection operators, i.e. operators $P : \mathcal{H}_{\text{total}} \to \mathcal{H}_{\text{total}}$, that satisfy $P^2 = P^\dagger = P$, with $(.)^\dagger$ denoting the matrix conjugate transposition operation. We

define a SL projection operator to be one which has a finite upper bound on the extent of its hopping elements:

Definition 1. An orthogonal projection operator $P : \mathcal{H}_{\text{total}} \to \mathcal{H}_{\text{total}}$ is said to be SL if there exists a finite integer b such that $\langle \vec{r}, i|P|\vec{r}\,', j\rangle = 0 \;\forall\; |\vec{r} - \vec{r}\,'| > b$ and $i, j \in \{1, \ldots, n\}$. The maximum hopping distance of P is the smallest integer b which satisfies this condition.

A wavefunction which has non-zero support only on a finite number of sites is said to be CS. Specifically,

Definition 2. A wavefunction is CS iff there exists a finite integer r, such that it has zero support outside a ball of radius r. The smallest integer value of r is called the size of the wavefunction. A basis is said to be a compactly supported orthogonal basis (CSOB) of (a finite) size R iff every constituent wavefunction is CS and has a size of at most R.

In the context of finite sized lattices, a basis is considered to be CS only if R is smaller than the size of the lattice. Similarly, only those projection operators that have a maximum hopping distance smaller than the size of the lattice will be considered to be SL.

For an SL projector P, the following notation will be used in the paper:

(a) Let $\Pi^P_{\vec{r}}$ denote the set of vectors obtained by operating P on all the orbitals at cell $\vec{r}$. That is,

$$\Pi^P_{\vec{r}} \coloneqq \{P|\vec{r}, i\rangle : i \in 1, \ldots, n\}. \tag{3}$$

The choice of which orbital basis is chosen while calculating $\Pi^P_{\vec{r}}$ will be specified, or will be clear from the context.

(b) Let $\mathcal{H}^P_{\vec{r}} \subset \mathcal{H}_{\text{total}}$ denote the space spanned by $\Pi^P_{\vec{r}}$.

(c) Let $\mathcal{H}^P \equiv \cup_{\vec{r}\in\mathbb{Z}^d} \mathcal{H}^P_{\vec{r}}$ denote the image of P.

(d) Let $\tilde{\Pi}^P_{\vec{r}}$ denote an orthonormal basis of $\mathcal{H}^P_{\vec{r}}$. ($\tilde{\Pi}^P_{\vec{r}}$ can be obtained by applying the Gram–Schmidt orthogonalization procedure on $\Pi^P_{\vec{r}}$). We note that since P is SL, all wavefunctions in the sets $\tilde{\Pi}^P_{\vec{r}}$ and $\Pi^P_{\vec{r}}$ are CS.

(e) Let $P_{\vec{r}}$ denote the orthogonal projection operator onto $\mathcal{H}^P_{\vec{r}}$. $P_{\vec{r}}$ can be expressed as

$$P_{\vec{r}} = \sum_{|\chi\rangle \in \tilde{\Pi}^P_{\vec{r}}} |\chi\rangle \langle\chi| . \tag{4}$$

2.2. Compactly supported Wannier functions and compact localized states

While the primary object of interest of this paper is CS WFs, a closely related type of basis consists of CS Wannier-type functions, which exist prominently in flat-band Hamiltonians. As we will show later, CS WFs' existence is related to the strict localization of the associated projector. While flat-band projectors need not be SL projectors and vice versa, both their images are spanned by CS Wannier-type functions and in some cases CS WFs as well. In this section, we will discuss these two types of bases for flat-band Hamiltonians and SL projectors.

Let us first discuss Wannier-type functions, which are in a sense a generalization of WFs. Similar to WFs, Wannier-type functions consist of a set of wavefunctions localized at a cell, and all their lattice translates, and span a band or a set of bands. However, unlike WFs which are by definition orthogonal, Wannier-type functions can be non-orthogonal, or even linearly dependent. Consequently, a set of m bands may be spanned by $l \geqslant m$ *flavors* of Wannier-type functions, whereas exactly m flavors of WFs span m bands. Wannier-type functions that are CS

[19, 20] are desirable in certain applications [15]. Importantly, the existence of non-orthogonal CS Wannier-type functions does not in general imply the existence of CS WFs.

CS Wannier-type functions exist most notably as bases spanning flat bands in flat-band Hamiltonians [21, 22]. Such functions corresponding to a flat band are also Hamiltonian eigenstates, and are also referred to as CLSs. In most flat-band Hamiltonians, the CLSs are not mutually orthogonal, and can even by linearly dependent. Indeed, in the presence of band touching, CLSs may not even span the entire flat band [41]. However, it is always possible to modify such models so that they have orthogonal CLSs spanning a flat band in an enlarged unit cell. This can be done by choosing a subset of CLSs, comprising regularly spaced CLSs with no physical overlap on the lattice [28, 29]. While such a set does not span a full band in a primitive cell representation, they always span an entire flat band in an appropriately enlarged unit cell. Hence, they can also be referred to as CS WFs. In some cases, flat-band Hamiltonians possess orthogonal CLSs naturally, without needing unit cell enlargement. Some popular examples from the literature with such bases are discussed in sections 3 and 4. It is possible to create many more examples of flat-band Hamiltonians with orthogonal CLSs, by constructing NN projectors as done in appendix A.2.

While the term CLSs is commonly used only in the context of flat-band Hamiltonians, the distinction between orthogonal CLSs and CS WFs is unnecessary for our purpose. Indeed, it is always possible to deform a band's energy without changing the subspace corresponding to it. Expressing a Hamiltonian as $H(\vec{k}) = \sum_i E_i(\vec{k})P_i(\vec{k})$, where P_i's are the band projectors, one can modify a band's energy function to 'flatten' the corresponding band [42] without modifying the band projectors, and vice versa. Such an operation does not affect the Wannier and Wannier-type functions spanning that band, since they are associated with the band subspace, and have no dependence on the band dispersion. Thus, (non-)orthogonal CLSs are a special type of CS Wannier(-type) functions. As a result, the conditions associated with the existence of orthogonal CLSs spanning a flat band, and those associated with the existence of CS WFs for any band which may or may not be flat, are equivalent to each other.

These arguments also highlight that the properties of the band projector are connected to the existence of CS WFs or orthogonal CLSs spanning a band. Indeed, as we will show later in the paper, the existence of CS WFs is tied to the band projector being SL. Like SL flat-band Hamiltonians, SL projectors also possess CS Wannier-type functions. In $1d$, they have the additional property that their images are spanned by CS WFs. Regardless of the dimension, non-orthogonal CLSs can be constructed straightforwardly for any SL projector. To that end, we first note that for any lattice vector $|\vec{r}, \alpha\rangle$, since $P^2 = P$,

$$P(P|\vec{r}, \alpha\rangle) = (P|\vec{r}, \alpha\rangle).$$

Thus, if $P|\vec{r}, \alpha\rangle \neq 0$, it is an eigenvector of P with eigenvalue 1. Since P is SL, $P|\vec{r}, \alpha\rangle$ is CS. Additionally, if P is TI, then the set $\{P|\vec{r}, \alpha\rangle | \vec{r} \in \mathbb{Z}^n\}$ is one flavor of CLS. If there are l number of α's for which $P|\vec{x}, \alpha\rangle \neq 0$, we obtain l number of CLSs which together span the band(s) corresponding to P. In general, without further processing, none of these wavefunctions are guaranteed to be mutually orthogonal. Moreover, it is possible for two wavefunctions within the same flavor of CLSs to be non-orthogonal to each other.

The existence of CS Wannier-type functions for SL projectors can be understood as a destructive interference phenomenon, similar to CLS in flat-band Hamiltonians. This is based on the rather simple observation that any SL projector can also be regarded as a flat-band Hamiltonian with two flat bands. The CLSs for the band with energy 1 are exactly the CS Wannier-type functions spanning the SL projector's image. Although gapped flat-bands are always spanned by a set of CLSs, they need not be orthogonal CLSs. Indeed, it is impossible

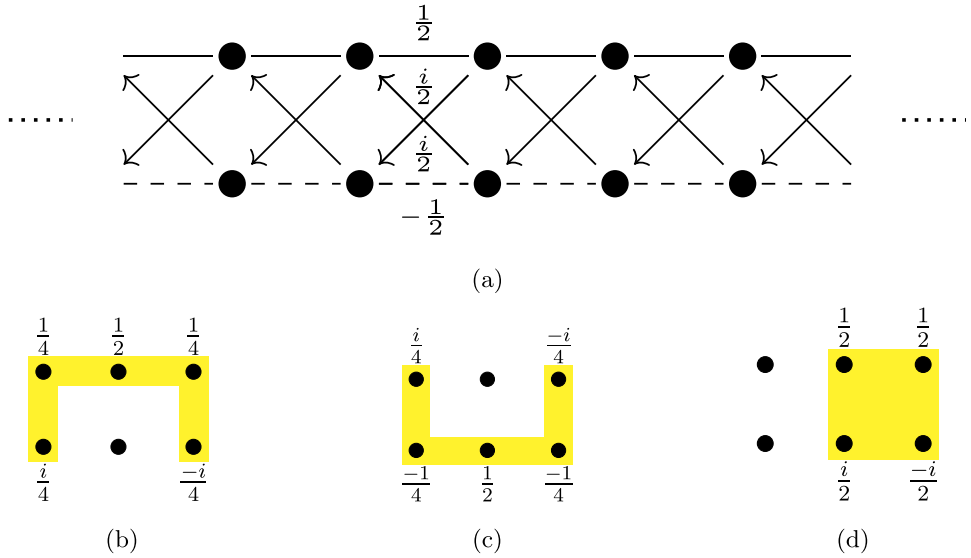

Figure 2. The real space connectivity of the projector from equation (5) is shown in (a). The upper and lower array of dots represent the two sublattices A and B respectively. An on-site potential of $\frac{1}{2}$ is present for each orbital. Two flavors of non-orthogonal CLSs, i.e. CS Wannier-type functions spanning the image of the projector are shown in (b) and (c). An orthogonal CLS, i.e. a CS Wannier function is shown in (d).

to find orthogonal CLSs spanning a flat-band for many flat-band Hamiltonians. Hence, interpreting an SL projector as a flat-band Hamiltonian does not directly help us to conclude that CS WFs spanning it exist. Especially in $1d$, this is a reflection of the fact that SL projectors are a subset of flat-band projectors. For some explicit examples of flat-band projectors that are not SL, see section 3 in reference [21].

We illustrate many of these points using a simple example of a $1d$ projector (see figure 2(a)), given by

$$P(k) = \frac{1}{2}\begin{pmatrix} 1+\cos k & \sin k \\ \sin k & 1-\cos k \end{pmatrix}. \tag{5}$$

We can construct two sets of CLSs by operating the projector on each A and B sublattice orbital (figures 2(b) and (c) show one CLS each from these two sets). Each set of CLS is not only non-orthogonal, but also linearly dependent, so that neither of the two sets span the image of the projector individually. However, both sets of CLSs considered together span the image of the projector, and hence form two flavors of CS Wannier-type functions. As we will show in the next section, one can always find CS WFs spanning the image of any $1d$ SL projector. For the example under consideration, this consists of the CLS shown in figure 2(d), and all its lattice translates. It can be easily verified that this set is orthogonal, and hence spans the image of P. While it is possible to also obtain these orthogonal CLSs using only destructive interference-based observations, it does not follow immediately that this can be done for projectors with more complicated connectivity, higher number of dimensions (for example, see (18)) or in the absence of lattice translation symmetry.

Thus, while it is clear that for any SL projector, one can construct non-orthogonal CLSs, it is far less obvious (and possibly untrue for $d > 1$) that one can construct orthogonal CLSs.

One of the objectives of this paper is to present a systematic procedure for the construction of such orthogonal CLSs/CS WFs, and the identification of conditions required for the existence of such functions.

Before proceeding, we note that for non-TI SL projectors, although CLSs as defined above do not exist, we may define an analogous basis. Specifically, the set $\{P|\vec{r},\alpha\rangle|\vec{r}\in\mathbb{Z}^d,\alpha=1,\ldots,n\}$ is a non-orthogonal basis of the image of P, and consists of CS wavefunctions.

2.3. Compact basis and strictly local projectors

The primary focus of this paper is the identification of necessary and sufficient conditions for the existence of a CSOB corresponding to a subspace. In this section, we prove the necessary condition for all dimensions: the strict locality of the associated orthogonal projector.

Proving that the span of a CSOB always corresponds to an SL projector is straightforward. Let a set S be a CSOB of size R on a d-dimensional lattice. Let P be the orthogonal projector onto the space spanned by S. Then for any two locations $z,z'\in\mathbb{Z}^d$ such that $|z-z'|>R$, and orbitals α,β, we note that

$$\begin{aligned}\langle z,\alpha|P|z',\beta\rangle &= \sum_{|\chi\rangle\in S}\langle z,\alpha|\chi\rangle\langle\chi|z',\beta\rangle\\ &= 0.\end{aligned}$$

In other words, the maximum hopping distance of P is at most R. By definition, P is then an SL projector.

Following a similar reasoning, we can easily show that if an orthogonal basis consists of wavefunctions each of which are CS along only one axis, then the corresponding projector is SL along that axis. This implies that if CS hybrid WFs exist for all choices of the localized axis, then the projector is SL (along all directions). This proves the necessary part of point (b) of the main result.

3. Compactly supported orthogonal basis: 1*d* lattices

As shown in section 2.3, it is straightforward to show that if a CSOB or a CS Wannier basis exists, then the corresponding projector is necessarily SL. In this section, we prove the converse, i.e. if a 1d projector is SL, then there exists a CSOB spanning its image, thereby completing the proof of part (a) of the main result. Specifically, we will show that

Theorem 1. *In 1*d *systems, the span of a set of occupied states possesses a CSOB if and only if the orthogonal projector onto the span is SL. Additionally:*

(*a*) *If the maximum hopping distance of an SL projector is* b*, then there exists such a basis consisting of wavefunctions of a maximum size of* $3b$ *cells, irrespective of the presence of translational invariance.*

(*b*) *If the projector is TI, its image is spanned by a CS Wannier basis in a size* $2b$ *supercell representation of the lattice.*

We prove these statements through algorithmic constructions of CSOBs and CS WFs, and provide bounds on their sizes on the way.

Let us briefly discuss some properties of SL projectors and outline the approach we will use in this section. We note that 1d SL projectors are band-diagonal matrices when expressed in the orbital basis (see figure 3). For example, every 1d NN projector can be represented by a block tridiagonal matrix, with the block size being equal to the number of orbitals per cell. Although

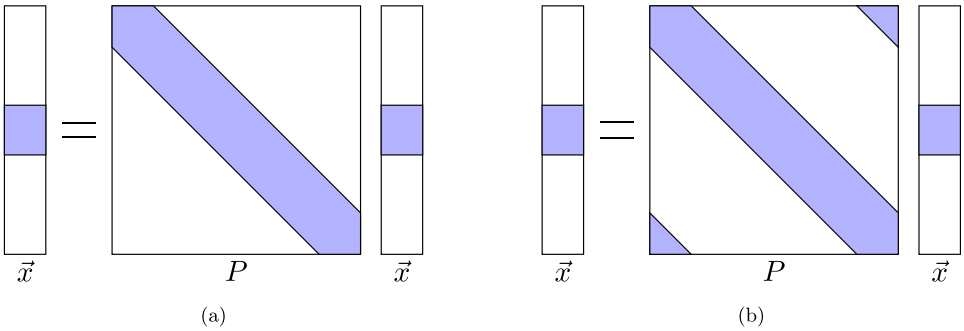

Figure 3. (a) SL projectors on $1d$ lattices are represented by band diagonal projection matrices, and CS wavefunctions are represented by sparse vectors which have non-zero components only within a finite patch (shown in blue). The main result for $1d$ projectors implies an orthogonal projection operator is band diagonal if and only if it possess a CS orthogonal eigenbasis. (b) $1d$ SL projectors on finite periodic lattices are band diagonal, with appropriate modifications at the corners. In theorem 1, a relation between the band width of the projector and the number of non-zero elements of the basis vectors is provided.

it is straightforward to obtain a CSOB for a block size of one, the corresponding statement is not obvious for larger block sizes. However, using the Gram–Schmidt orthogonalization procedure with an appropriate orthogonalization sequence, we show that it is always possible to obtain such an eigenbasis for any block size (see section 3.1). If the projector is also TI, i.e. with repeating blocks in the matrix representation, the basis can be chosen to be a Wannier basis in a supercell representation (see section 3.2). We then extend these results to all $1d$ SL projectors, since they can be represented as NN projectors using supercell representations (see section 3.3). In terms of matrices, this is equivalent to expressing any band diagonal matrix as a block-tridiagonal matrix by grouping together the original blocks into appropriate larger blocks. In this sense, the problem of obtaining a CSOB for any SL projector is equivalent to the problem of obtaining one for an NN projector.

While a number of model Hamiltonian systems possessing CS WFs and orthogonal CLSs have been studied in the literature, to our knowledge, this is the first time that the connection of such systems with the strict localization of the corresponding projection operator has been explicitly established. Most examples from the literature with CS WFs involve flat-band Hamiltonians defined on the Creutz ladder [43], the sawtooth lattice [28, 29] and the diamond lattice [44]. Here, we briefly discuss the Creutz lattice, which has been extensively studied both theoretically [45–47] and experimentally [48, 49]. As noted in [47], for one choice of parameters (see figure 4), the Creutz ladder has two exactly flat bands of energies $\pm 2t$, each of which is spanned by CS WFs. The corresponding Hamiltonian in k-space is given by:

$$H(k) = 2t \begin{pmatrix} \sin k & \cos k \\ \cos k & -\sin k \end{pmatrix}. \tag{6}$$

As mentioned in section 2.2, SL flat-band Hamiltonians possess some destructive interference properties, which constrain the movement of initially localized particles. For example, in the system under consideration, a particle initially localized on an A orbital cannot diffuse to a B orbital located more than a hop away (see figure 2 and related discussion in reference [47]). Based on this observation, one can obtain orthogonal CLSs, or equivalently, CS WFs for the two bands of this Hamiltonian. The WFs (labeled by $\pm$ for the two bands) localized at cell z

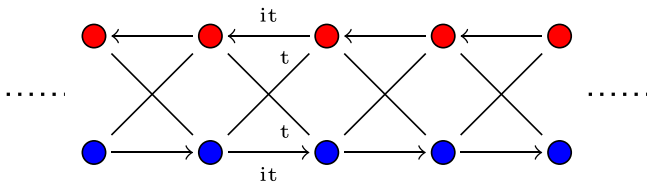

Figure 4. Example of a popular model with CS WFs: the Creutz ladder. The hopping amplitudes result in two flat bands and CS WFs. The A (B) orbitals are shown in red (blue). The hopping amplitudes are shown next to the arrows.

are given by:

$$|W_{\pm}\rangle = \frac{1}{2}\left(\pm i|z,A\rangle \pm |z,B\rangle + |z+1,A\rangle + i|z+1,B\rangle\right).$$

In accordance with the predictions of our paper, the band projectors onto the two bands are SL, and are given by

$$P_{\pm}(k) = \frac{1}{2}\begin{pmatrix} 1 \pm \sin k & \pm\cos k \\ \pm\cos k & 1 \mp \sin k \end{pmatrix}. \tag{7}$$

Indeed, using the techniques developed in the next subsection, one can obtain these CS WFs from the expressions for the projectors $P_{\pm}(k)$.

While most popular flat-band Hamiltonians do not possess CS WFs, i.e. a set of orthogonal CLSs spanning the flat band, as discussed in section 2.2, it is possible to construct models with orthogonal CLSs by enlargement of the unit cell of any known flat-band model. This was done for example in [28, 29] to obtain CS WFs spanning a flat band in the sawtooth lattice.

Although most of the examples from the literature involve flat bands, CS WFs and SL projectors can correspond to dispersive bands. Such an example is provided in appendix A.1, along with a discussion of the CS WFs obtained using the algorithm from the next subsection.

3.1. Nearest neighbor projectors

In this section, we present an algorithm for obtaining a CSOB corresponding to any NN projector. The algorithm is based on the Gram–Schmidt orthogonalization procedure, and produces a CSOB with each basis vector having a maximum spatial extent of 3 consecutive lattice cells. The methods in this section are applicable even if the projector is not TI.

The basic idea underlying our procedure is to obtain the set $\tilde{\Pi}_z^P$ defined in section 2.1, corresponding to the localized eigenstates of P_z for some lattice site z, and to 'reduce' P to $P - P_z$ as required by the Gram–Schmidt procedure. Then, we operate this reduced projector $P - P_z$ on another cell z', and iterate along a sequence of cell locations which includes all the integers. The union of all the $\tilde{\Pi}_z^P$ sets will form an orthonormal basis for the image of P. While at the first step, $\tilde{\Pi}_z^P$ is guaranteed to have CS wavefunctions, it is not obvious that the size of the corresponding wavefunctions stays bounded for subsequent steps. With the help of the following lemma, we can show that the size of each vector at any step will be at most three consecutive cells.

Lemma 1. *For any $z \in \mathbb{Z}$, orbital indices $i,j \in \{1,\ldots,n\}$, and integers $\delta,\delta' > 0$,*

$$\langle z-\delta, i|(P - P_z)|z+\delta', j\rangle = 0. \tag{8}$$

Additionally,

$$(P - P_z)|z, j\rangle = 0. \tag{9}$$

Proof. For any cell z, let $P_{zz} : \mathcal{H}^z \to \mathcal{H}^z$ denote the $n \times n$ matrix corresponding to the matrix elements of P between different orbitals at cell z, i.e.

$$(P_{zz})_{ij} = \langle z, i|P|z, j\rangle.$$

Since P is Hermitian, P_{zz} is also Hermitian. Hence, there exists a unitary matrix U_z, such that $D_z = U_z^\dagger P_{zz} U_z$ is a real diagonal matrix. Let d_z denote the vector of diagonal elements of the matrix D_z. The unitary U_z defines a new basis at z:

$$|z, i\rangle' := \sum_j (U_z)_{ji} |z, j\rangle. \tag{10}$$

We call the orbital basis $\{|z, \alpha\rangle' | \alpha = 1, \ldots, n\}$ a diagonal basis at z. Since $\langle z, i|'P|z, j\rangle' = d_i \delta_{ij}$, we can significantly reduce the intra-cell connectivity of P, by performing the unitary transformation at every cell separately. Equivalently, we use the global unitary transformation

$$U := \bigoplus_{z \in \mathbb{Z}} U_z. \tag{11}$$

Hereafter, for notational convenience, we drop the prime outside the vectors, and assume that we have already rotated the basis to a diagonal one. Thus, $\langle z, \alpha|P|z, \beta\rangle = 0$ whenever $\alpha \neq \beta$.

Now we obtain a few important identities using the fact that P is an orthogonal NN projector, and using appropriate insertions of resolution of identity:

(a) Since P is positive-semidefinite, for any cell z and orbital α, we have

$$\langle z, \alpha|P|z, \alpha\rangle \geqslant 0. \tag{12}$$

(b) For any two neighboring cells z and $z + 1$ and orbitals α, β, we have

$$\langle z, \alpha|P|z, \alpha\rangle + \langle z + 1, \beta|P|z + 1, \beta\rangle = 1, \quad \text{whenever } \langle z, \alpha|P|z + 1, \beta\rangle \neq 0. \tag{13}$$

This follows from

$$\begin{aligned}
\langle z, \alpha|P|z + 1, \beta\rangle &= \langle z, \alpha|P^2|z + 1, \beta\rangle \\
&= \langle z, \alpha|P|z, \alpha\rangle \langle z, \alpha|P|z + 1, \beta\rangle + \langle z, \alpha|P|z + 1, \beta\rangle \\
&\quad \times \langle z + 1, \beta|P|z + 1, \beta\rangle \\
&= \langle z, \alpha|P|z + 1, \beta\rangle \left(\langle z, \alpha|P|z, \alpha\rangle + \langle z + 1, \beta|P|z + 1, \beta\rangle \right).
\end{aligned}$$

(c) Similarly, for any two cells z and $z + 2$ separated by two hops, since P is an NN operator,

$$\sum_\gamma \langle z, \alpha|P|z + 1, \gamma\rangle \langle z + 1, \gamma|P|z + 2, \beta\rangle = 0. \tag{14}$$

Now we obtain the projector P_z by orthogonalizing Π_z (using the diagonal basis orbitals of P_{zz} in expression 3). Since $\langle z, \alpha|P|z, \beta\rangle = 0$ whenever $\alpha \neq \beta$, Π_z is already orthogonal, so

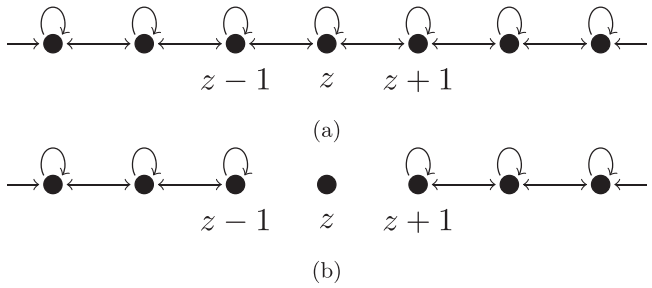

Figure 5. Change in the connectivity of an NN projector after a Gram–Schmidt step. Each dot represents a cell, with arrows indicating possible non-zero matrix elements of P. (a) Connectivity of an NN projector P. (b) Connectivity of the reduced projector $P - P_z$. Missing arrows indicate that the corresponding matrix elements are zero.

we only need to normalize the vectors in it in order to obtain an orthonormal set. Whenever $P|z,\alpha\rangle \neq 0$, we denote the corresponding normalized vector by

$$|P,z,\alpha\rangle := \frac{P|z,\alpha\rangle}{\sqrt{\langle z,\alpha|P|z,\alpha\rangle}}.$$

Thus, we obtain P_z by adding the projector onto each orthonormal vector:

$$P_z \equiv \sum_{\alpha}^{(d_z)_\alpha \neq 0} |P,z,\alpha\rangle\langle P,z,\alpha| = \sum_{\alpha}^{(d_z)_\alpha \neq 0} P\frac{|z,\alpha\rangle\langle z,\alpha|}{\langle z,\alpha|P|z,\alpha\rangle}P.$$

Since Π_z consists of wavefunctions with non-zero support only on cells z and $z \pm 1$, equation (8) is already satisfied, whenever $\delta > 1$ or $\delta' > 1$. Thus, we only need to verify that (8) is satisfied for $\delta = \delta' = 1$, for which, we get

$$\langle z-1,\alpha|P_z|z+1,\beta\rangle = \sum_{\gamma}^{(d_z)_\gamma \neq 0} \frac{\langle z-1,\alpha|P|z,\gamma\rangle\langle z,\gamma|P|z+1,\beta\rangle}{\langle z,\gamma|P|z,\gamma\rangle}.$$

Any non-zero term in the summation will have $\langle z-1,\alpha|P|z,\gamma\rangle \neq 0$. From condition (13), all such orbitals γ at cell z possess the same self-hop:

$$\langle z,\gamma|P|z,\gamma\rangle = 1 - \langle z-1,\alpha|P|z-1,\alpha\rangle \neq 0.$$

Thus, we get

$$\begin{aligned}\langle z-1,\alpha|P_z|z+1,\beta\rangle &= \frac{1}{1-\langle z-1,\alpha|P|z-1,\alpha\rangle}\sum_{\gamma}\langle z-1,\alpha|P|z,\gamma\rangle\langle z,\gamma|P|z+1,\beta\rangle \\ &= 0, \end{aligned} \tag{15}$$

where we have used condition (14). Since P has vanishing matrix elements between orbitals lying on opposite sides of z, this proves equation (8).

We note that $P|z,\alpha\rangle = P_z|z,\alpha\rangle$ and hence $(P - P_z)|z,\alpha\rangle = 0$. This leads to equation (9). The connectivity of the reduced projector is shown in figure 5. □

Procedure 1. Procedure for constructing a CSOB for the image of any $1d$ NN projector.

Input: an NN projector $\mathcal{P}$ acting on a $1d$ lattice
Procedure: define a non-repeating sequence $S \equiv z_0, z_1, \ldots$ of integers, s.t. it contains all the integers.
Set $P \leftarrow \mathcal{P}$. Initialize $k = 0$, and do:

1. Set $z \leftarrow z_k$
2. Obtain Π_z^P (as defined in equation (3))
3. Orthonormalize the set Π_z^P to obtain $\tilde{\Pi}_z^P$
4. Obtain P_z from $\tilde{\Pi}_z^P$ using (4)
5. Update $P \leftarrow P - P_z$, increment k, and go back to step (1)

Output: the set $\tilde{\Pi} := \cup_{z\in\mathbb{Z}} \tilde{\Pi}_z^P$ of CS wavefunctions, which is an orthonormal basis of the image of the projector $\mathcal{P}$

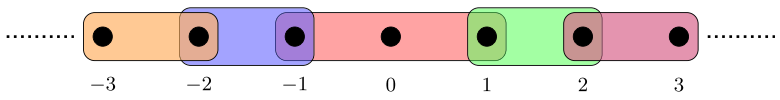

Figure 6. If we use the sequence $S = 0, -1, 1, -2, 2, \ldots$ in procedure 1, then all sets $\tilde{\Pi}_z^P$ except for $\tilde{\Pi}_0^P$ consist of wavefunctions of a maximum size of 2. Each colored rectangle represents the maximum spatial extent of the wavefunctions in $\tilde{\Pi}_z^P$ obtained during one iteration of the procedure. Each unit cell is represented by a black dot.

Based on this lemma, we present a method for obtaining a CSOB for the image of an NN projector, as described in procedure 1.

Lemma 2. *The set $\tilde{\Pi}$ obtained from the Gram–Schmidt procedure 1 is an orthonormal basis of the image of the NN projector $\mathcal{P}$. Furthermore, every element of $\tilde{\Pi}$ is CS, with a spatial extent of no more than three consecutive cells.*

Proof. The set $\cup_z \Pi_z^P$ spans the image of $\mathcal{P}$. Hence, procedure 1, which is the application of the Gram–Schimidt procedure on it, creates an orthonormal basis of the image of $\mathcal{P}$. Lemma 1 implies that the reduced projector $P - P_z$ obtained at any iteration in the procedure is also an NN projector. Thus, every vector belonging to $\tilde{\Pi}_z^P$ for any z is guaranteed to be CS, with a maximum spatial extent of 3 consecutive cells. □

It is possible to choose a sequence S so that at most n of the created basis vectors have a spatial extent of 3 cells, with all the remaining vectors having a spatial extent of at most 2 consecutive cells. For an example, see figure 6.

3.2. Translationally invariant nearest neighbor projectors

Although procedure 1 from the previous section also works for TI projectors, in general, the obtained basis may not consist of WFs. In this section, we will show that it is possible to obtain a Wannier basis consisting of CS functions for the image of P, in a size 2 supercell lattice representation. By a size 2 supercell representation of the lattice, we mean relabeling the cells so that the lattice is regarded as consisting of 'supercells' which are each twice the size of the original cell. In this representation, the unit cell is the supercell which consists of two primitive unit cells. (We also use a supercell representation for the conversion of an SL projector to an NN projector, as will be discussed in the next subsection.) To that end, we first divide the lattice into two subsets, A, and B, consisting of alternating cells. For concreteness, we choose A to consist of even locations ($2\mathbb{Z}$), and B to be the odd locations ($2\mathbb{Z} + 1$).

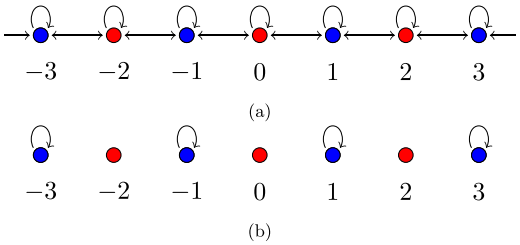

Figure 7. Sets A and B are shown in red and blue respectively. (a) Connectivity of an NN projector P. (b) Connectivity of $P - P_A$. Missing arrows indicate vanishing matrix elements.

We define the set Π_A^P as being

$$\Pi_A^P = \bigcup_{i\in A} \Pi_i^P.$$

We also define $\mathcal{H}_A^P$ to be the span of Π_A^P, and P_A to be the orthogonal projection onto $\mathcal{H}_A^P$. From lemma 1, we note that $P - P_A$ has a significantly reduced connectivity, as shown in figure 7. Specifically, the only non-zero matrix elements of $P - P_A$ between any two orbitals, are those between any two orbitals located at the same cell belonging to set B.

Since P is TI, it is useful to define a translation operator $\widehat{\mathcal{T}}$, which satisfies

$$\widehat{\mathcal{T}}|z, i\rangle = |z+1, i\rangle,$$

for all $z \in \mathbb{Z}$ and $i \in \{1, \ldots, n\}$. Since P is TI, $P = \widehat{\mathcal{T}}^\dagger P \widehat{\mathcal{T}}$.

The algorithm for obtaining a CSOB is summarized in procedure 2.

Lemma 3. *The output obtained using procedure 2 is a CS Wannier basis spanning the image of P corresponding to a size 2 supercell representation.*

Proof. The output of procedure 2 is the set $\tilde{\Pi}$, which is a union of two disjoint sets (see equation (16)). The first set is a union of the set $\tilde{\Pi}_0^P$, and all its even unit cell translates. We will now show that this set is an orthogonal basis of $\mathcal{H}_A^P$.

First, we note that the set $\{\widehat{\mathcal{T}}^{2z}|\chi\rangle : |\chi\rangle \in \tilde{\Pi}_0^P\}$ is an orthogonal basis of $\mathcal{H}_{2z}^P$, since P is TI. Moreover, for any $z \neq 0$, this set is also orthogonal to the set $\tilde{\Pi}_0^P$. To see this, we show that *any* orthonormal bases $\tilde{\Pi}_{z_1}^P$ and $\tilde{\Pi}_{z_2}^P$ for distinct locations $z_1, z_2 \in A$ are mutually orthogonal. Let $|\Psi\rangle \in \mathcal{H}_{z_1}^P$ and $|\Phi\rangle \in \mathcal{H}_{z_2}^P$ be two vectors. There exist vectors $|\psi\rangle \in \mathcal{H}^{z_1}$ and $|\phi\rangle \in \mathcal{H}^{z_2}$ such that $|\Psi\rangle = P|\psi\rangle$ and $|\Phi\rangle = P|\phi\rangle$. Taking the inner product of $|\Psi\rangle$ and $|\Phi\rangle$, we obtain

$$\langle\Phi|\Psi\rangle = \langle\phi|P^\dagger P|\psi\rangle = \langle\phi|P|\psi\rangle = 0,$$

since z_1 and z_2 are located at least two hops away, which is larger than the maximum hopping distance of P. Thus, $\mathcal{H}_{z_1}^P$ and $\mathcal{H}_{z_2}^P$ are mutually orthogonal for distinct $z_1, z_2 \in A$. Thus, the set $\bigcup_{z\in\mathbb{Z}}\{\widehat{\mathcal{T}}^{2z}|\chi\rangle : |\chi\rangle \in \tilde{\Pi}_0^P\}$ is an orthogonal basis of $\mathcal{H}_A^P$. Additionally, since P is NN hopping, it consists of CS wavefunctions with a maximum spatial extent of 3 cells, as shown in figure 8(a).

Procedure 2. CS Wannier basis for 1*d* TI NN projectors.

Input: a 1*d* TI NN projection operator P

Procedure:

1. Obtain Π_0^P, and orthogonalize it to obtain the set $\tilde{\Pi}_0^P$
2. Obtain the orthogonal projection operator P_0 onto the span of Π_0^P
3. Obtain a reduced projection operator $P' \coloneqq P - P_0 - \widehat{\mathcal{T}}^2 P_0 \widehat{\mathcal{T}}^{\dagger 2}$
4. Obtain and orthogonalize $\Pi_1^{P'}$ to obtain the set $\tilde{\Pi}_1^{P'}$
5. Obtain the set $\tilde{\Pi}$, defined as

$$\tilde{\Pi} = \left(\bigcup_{z\in\mathbb{Z}} \{\widehat{\mathcal{T}}^{2z}|\chi\rangle : |\chi\rangle \in \tilde{\Pi}_0^P\}\right) \cup \left(\bigcup_{z\in\mathbb{Z}} \{\widehat{\mathcal{T}}^{2z}|\chi\rangle : |\chi\rangle \in \tilde{\Pi}_1^{P'}\}\right). \tag{16}$$

Output: the set $\tilde{\Pi}$ consisting of CS WFs spanning the image of P, corresponding to a size 2 supercell representation.

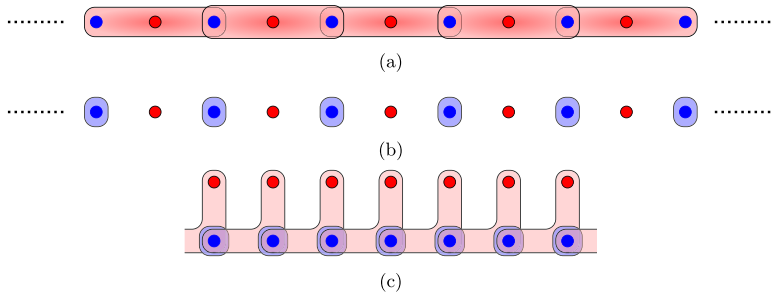

Figure 8. The red and blue dots denote the lattice sites belonging to sets A and B respectively. (a) Wavefunctions in $\tilde{\Pi}_z^P$ centered at cell $z \in A$ are chosen to be the wavefunctions in $\tilde{\Pi}_0^P$ translated by z cells. Each red rectangle centered at z denotes the maximum spatial extent of wavefunctions belonging to $\tilde{\Pi}_z^P$. (b) Each blue bubble denotes the maximum spatial extent of the wavefunctions in the set $\tilde{\Pi}_1^{P-P_A}$, and its translates by an even number of cells. (c) The two sets of functions together form a Wannier basis in a size 2 supercell representation, with each supercell consisting of one cell each from A and B.

The second set in equation (16) is an orthonormal basis of $\mathcal{H}^P \backslash \mathcal{H}_A^P$. To prove this, we first note that

$$P'|1,i\rangle = (P - P_0 - \widehat{\mathcal{T}}^2 P_0 \widehat{\mathcal{T}}^{\dagger 2})|1,i\rangle = \left[P - \left(\sum_{z\in\mathbb{Z}} \widehat{\mathcal{T}}^{2z} P_0 \widehat{\mathcal{T}}^{\dagger 2z}\right)\right]|1,i\rangle$$
$$= (P - P_A)|1,i\rangle.$$

Hence, the set $\tilde{\Pi}_1^{P'}$ is an orthonormal basis of $\mathcal{H}_1^{P-P_A}$. $P - P_A$ remains invariant under translations by an even number of cells. Since $P - P_A$ is also a NN projector (using lemma 1), using the same arguments as for the first set, we conclude that $\bigcup_{z\in\mathbb{Z}}\{\widehat{\mathcal{T}}^{2z}|\chi\rangle : |\chi\rangle \in \tilde{\Pi}_1^{P'}\}$ is an orthogonal basis of $\mathcal{H}^P \backslash \mathcal{H}_A^P$. Additionally, using lemma 1, we infer that every wavefunction it contains is CS, with non-zero support on only one cell (see figure 8(b)).

Thus, $\tilde{\Pi}$ is a CS orthogonal basis of $\mathcal{H}^P$. By construction,

$$\widehat{\mathcal{T}}^{2z}|\chi\rangle \in \Pi \quad \text{if } |\chi\rangle \in \tilde{\Pi},$$

for any $z \in \mathbb{Z}$. Thus, $\tilde{\Pi}$ consists of CS Wannier basis, within a size 2 supercell representation (figure 8(c)). □

3.3. *Supercell representation and strictly local projectors*

As discussed at the beginning of this section, an SL operator on a $1d$ lattice with a maximum hopping distance b can be expressed as an operator with only NN hopping terms using a supercell representation with each supercell consisting of b number of primitive cells (for an illustrative example, see figure 9). The range of the operator is reduced, at the cost of an increase in the number of orbitals per cell ($n \to nb$). This transformation enables us to apply the techniques and results for NN projectors ($b = 1$) to SL projectors ($b \geqslant 1$).

In particular, if we choose the supercell located at the origin to consist of primitive cells $0, 1, \ldots, b-1$, the position and orbital indices in the two representations have the following

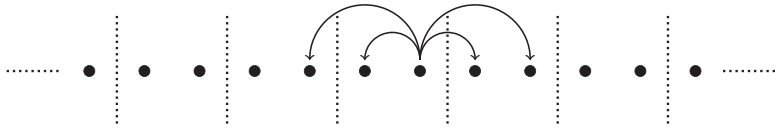

Figure 9. An example of conversion of a 1*d* SL operator to an NN operator using a supercell representation. If an operator has a maximum hopping distance of 2, then grouping the sites in pairs converts the operator to an NN operator in the 'supercell' representation.

correspondence:

$$\begin{aligned} &\text{Primitive cell} \longleftrightarrow \text{Supercell} \\ &|z,i\rangle \;\equiv\; |z\backslash b, n \times (z \bmod b) + i\rangle_s, \end{aligned} \tag{17}$$

with the subscript s denoting a vector in the supercell representation, and $\backslash$ denoting the quotient upon division.

Putting together the results from the previous subsections and the conversion of an SL projector to an NN projector using the supercell representation, we arrive at the following results for arbitrary range SL projectors.

Corollary 1. *The image of an SL projector on a 1*d *lattice with a maximum hopping distance b possess a CSOB consisting of wavefunctions of a maximum spatial extent of* 3*b consecutive cells.*

We first create a size b supercell representation where P is an NN projector. Using procedure 1, we obtain a CSOB in this supercell representation. We revert back to the original, or primitive cell representation using the correspondence (17). This process is summarized in the following sequence:

Primitive cell representation $\rightarrow$		Supercell representation	$\rightarrow$ Primitive cell representation
SL projector ($b \geqslant 1$)	$\rightarrow$ NN projector ($b = 1$)	$\xrightarrow{\text{Procedure 1}}$	CSOB (max size 3) $\rightarrow$ CSOB (max size $3b$)

Similarly, we can use procedure 2 for obtaining a Wannier basis for arbitrary range TI SL projectors.

Corollary 2. *The image of a TI SL projector with a maximum hopping distance b on a 1*d *lattice is spanned by a CS Wannier basis within a size* 2*b supercell lattice representation.*

The procedure for obtaining such a basis is summarized in the following sequence:

Primitive cell representation	$\xrightarrow{\text{Size } b}$	Size b supercell representation	$\xrightarrow{\text{Size 2}}$	Size $2b$ supercell representation
SL projector ($b \geqslant 1$)	$\rightarrow$	NN projector ($b = 1$)	$\xrightarrow{\text{Procedure 2}}$	CS Wannier basis

To summarize, we have shown that the image of a SL projector in 1*d* is always spanned by a CS orthogonal basis (or a CS Wannier basis if the projector has lattice translational invariance). This completes our proof of theorem 1.

Having presented a technique for the construction of CS WFs for 1*d* SL projectors, we apply this technique to an example Hamiltonian with a band associated with an SL projector in appendix A.1. Furthermore, we discuss why the Gram–Schmidt orthogonalization procedure

in our algorithm is easier to use instead of the symmetric orthogonalization procedure [50]. We also compare our results with those obtained using the maximally localized WFs procedure [11].

In the next section we will study how these results can be extended to higher dimensional lattices which have a larger coordination number. We close this section with some comments on the Bethe lattice which is sometimes regarded as an infinite dimensional lattice. For an NN projector on the Bethe lattice with an arbitrary coordination number, using the methods of lemma 1, we can show that projecting out a site results in a reduced connectivity for the projector. Consequently, analogous to lemma 3 and procedure 1, using an arbitrary sequence of site locations guarantees the creation of an orthonormal basis which is CS.

4. Higher dimensional lattices

In $1d$, we were able to show that for an arbitrary basis of wavefunctions, the existence of a CSOB equals the strict locality of the associated projector. However, the results for the $1d$ case do not all carry over to higher dimensional lattices. While strict locality of the projector is a necessary condition for the existence of a CSOB even in higher dimensions (see section 2.3), the methods we have employed so far for the $1d$ case do not prove that it is a sufficient one. Our proof for the existence of a CSOB given any $1d$ SL projector relied on the fact that any $1d$ SL projector can be represented as a nearest-neighbor (NN) projector in a supercell representation, or equivalently, a block tridiagonal matrix in the orbital basis. In higher dimensions, such a simple matrix representation for even the simplest non-trivial SL projector, i.e. an NN projector is lacking. Generic SL or NN projectors in $d > 1$ cannot be represented by block tridiagonal matrices, or even band diagonal matrices. This makes the task of identifying the properties of a projector that are equivalent to the existence of a CSOB difficult.

Consequently, we identify a condition more stringent than strict locality of the projector as a sufficient condition for the existence of a CSOB. While NN projectors in $d > 1$ cannot in general be represented as block tridiagonal matrices, it is still possible to show that the image of any NN projector is spanned by a CSOB. However, unlike in $1d$, higher dimensional SL projectors cannot in general be expressed as NN projectors using a supercell transformation. Consequently, we can extend the results for NN projectors only to those SL projectors that can be brought to an NN form using a supercell representation. We call such projectors NN-reducible projectors. (For a discussion of the condition of being NN-reducible, we refer the reader to section 4.4.) Due to these considerations, unlike in $1d$, we obtain separate necessary and sufficient conditions for the existence of a CSOB spanning a subspace. Since the necessary condition has already been proved in section 2.3, in this section, we focus on proving the sufficient condition, which is that a projector should be NN hopping, or NN-reducible.

Additionally, as mentioned in the introduction, in higher dimensional lattices it is possible to construct 'hybrid WFs' that are CS along just one dimension. We show that their existence hinges on the strict locality of projectors just like the existence of CS wavefunctions in one dimension.

For all these cases, we provide algorithms for obtaining CSOBs and CS hybrid WFs, and provide upper bounds on their sizes. In summary, we will prove the following statements.

Theorem 2. *Let P be a SL projector with a maximum hopping distance b, acting on a $d > 1$ dimensional tight binding lattice.*

(*a*) *If P is NN reducible, there exists a CS orthonormal basis spanning its image, with each basis vector having a size of at most $3b \times \ldots \times 3b$ cells.*

(*b*) *If P is TI and NN reducible, there exists a CS Wannier basis spanning its image, in a size* $2b \times \ldots \times 2b$ *supercell lattice representation.*

(*c*) *If P is TI, its image is spanned by hybrid WFs which have compact support along the localized* (*i.e. Wannier-like*) *dimension, in a size* $2b$ *supercell representation of the lattice. The supercell transformation is required only along the localized dimension, which may be chosen to be any of the d dimensions. Moreover, if P is SL along any one direction with a maximum hopping distance b*, (*with no restrictions on the localization along the other directions*), *then SL hybrid WFs corresponding to a size* $2b$ *supercell which are localized along that direction can be formed.*

In addition, we will discuss the topological properties of such projectors in this section.

Before proving these statements, we first discuss some model Hamiltonians with CS WFs. In figure 10, we show two examples from the literature of $2d$ flat-band Hamiltonians, that have flat bands spanned by orthogonal CLSs, i.e. flat-band CS WFs. These Hamiltonians are based on the square Kagome lattice [45, 51] with six sites per unit cell and the frustrated bilayer [52, 53] with two sites per unit cell. In both cases the natural choices of the primitive cells are such that each CLS lies entirely within a unit cell. While CS WFs can be easily constructed for the flat bands in these examples, for many flat-band Hamiltonians, orthogonal CLSs spanning a flat band do not exist. However, as discussed in section 2.2, it is possible to modify such Hamiltonians by enlargement of the unit cell, so that orthogonal CLSs span an entire flat band. This approach was used for example in reference [45], to construct two Hamiltonians on the Kagome lattice wherein a flat band is spanned by CS WFs. One can apply the same technique to other flat-band models from the literature, such as the decorated square lattice [54] and the dice lattice [55].

In all of these examples, the CS WFs are associated with flat bands, and are localized within one cell each. Consequently, the corresponding band projector is on-site hopping, and hence is independent of k in a k-space representation. One can simply diagonalize the projector in order to obtain CS WFs in such cases. However, there are many Hamiltonians with a band spanned by CS WFs that are spread across multiple cells, and with band projectors that are SL, but not on-site hopping. While one can diagonalize a TI NN projector expressed in k-space, in general a Fourier transform of the obtained Bloch wavefunction results in exponentially localized WFs as opposed to CS WFs (for an example, see appendix A.1). Similarly, as discussed in section 2.2, it may be possible to construct CS WFs using destructive interference arguments for TI NN projectors if they have a simple form. However, it is not straightforward to do so for a more complicated projector, such the following $2d$ NN projector:

$$P(k) = \frac{1}{12}\begin{pmatrix} e^{-iky}\sqrt{3}+e^{iky}\sqrt{3}+6 & -e^{-iky}\sqrt{3}+e^{iky}\sqrt{3}+2e^{ikx}-2 & e^{-iky}\sqrt{3}+2e^{ikx}+1 & -e^{iky}\sqrt{3}+2e^{ikx}+1 \\ e^{-iky}\sqrt{3}-e^{iky}\sqrt{3}+2e^{-ikx}-2 & -e^{-iky}\sqrt{3}-e^{iky}\sqrt{3}+6 & e^{-iky}\sqrt{3}-2e^{-ikx}-1 & e^{iky}\sqrt{3}+2e^{-ikx}+1 \\ e^{iky}\sqrt{3}+2e^{-ikx}+1 & e^{iky}\sqrt{3}-2e^{ikx}-1 & 7-2e^{-ikx}-2e^{ikx} & e^{-ikx}\left(-e^{i(kx+ky)}\sqrt{3}-2\,e^{2ikx}+2\right) \\ -e^{-iky}\sqrt{3}+2e^{-ikx}+1 & e^{-iky}\sqrt{3}+2e^{ikx}+1 & -e^{-iky}\sqrt{3}-2e^{-ikx}+2e^{ikx} & 5+2e^{-ikx}+2e^{ikx} \end{pmatrix}. \tag{18}$$

In contrast, the method presented in this section enables us to construct CS WFs since this projector is NN hopping. The WFs (centered at (x, y)) so obtained are $|W_1\rangle = \frac{1}{\sqrt{6}}|x, y\rangle \otimes (|B\rangle + |C\rangle + |D\rangle) + \frac{1}{\sqrt{6}}|x+1, y\rangle \otimes (|A\rangle - |C\rangle + |D\rangle)$ and $|W_2\rangle = \frac{1}{2}|x, y\rangle \otimes (|A\rangle - |B\rangle + |C\rangle) + \frac{1}{2\sqrt{3}}|x, y-1\rangle \otimes (|A\rangle + |B\rangle - |D\rangle)$, where the orbitals are labeled by letters A to D.

Having discussed some examples, we proceed to the proof of theorem 2, which we split across the following subsections. Since the problem of finding hybrid WFs can be reduced to

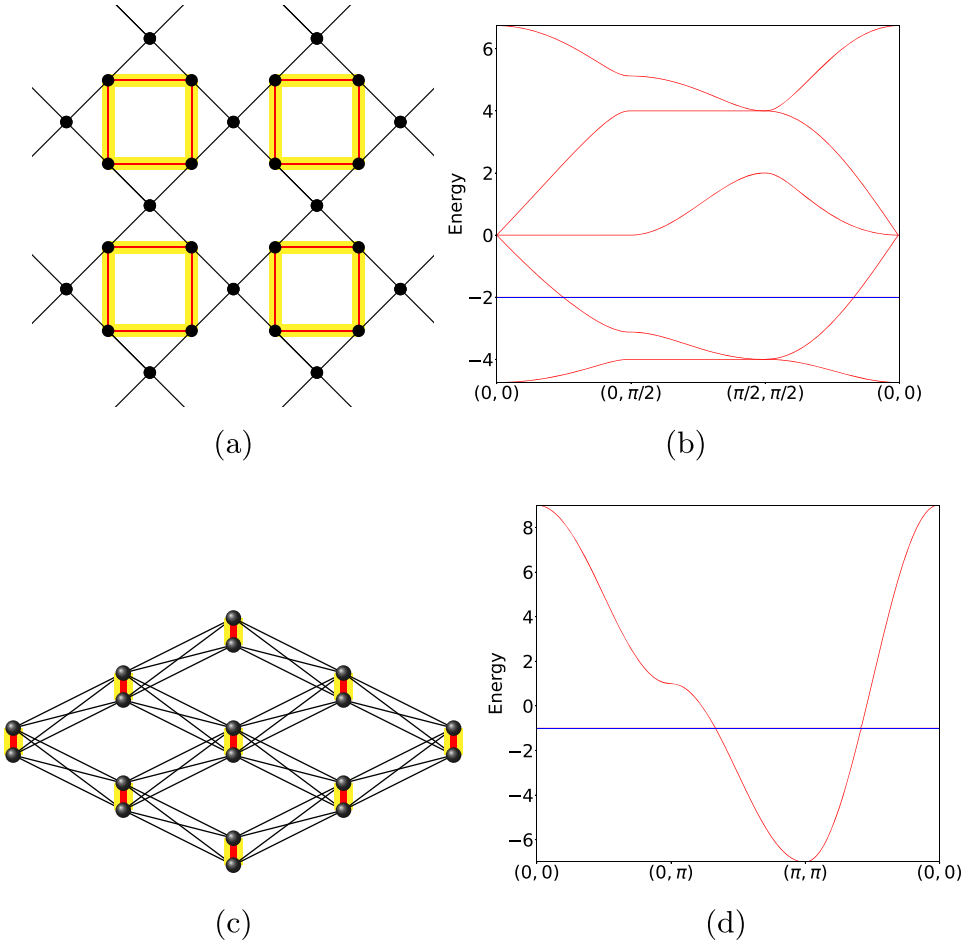

Figure 10. (a) The square Kagome lattice and (c) the frustrated bilayer lattice. In both cases, the black and red segments denote hopping elements with values t_1 and t_2 respectively. The flat band CLSs, i.e. CS WFs are highlighted in yellow. In the case of the square Kagome lattice, each CLS has support on four sites and an amplitude of $\frac{1}{2}$ with alternating signs on the four sites. For the frustrated bilayer lattice, each CLSs has an amplitude of $+1$ and -1 on the two sites where it is located. The band structures of the square Kagome lattice with $(t_1, t_2) = (2, 1)$, and of the frustrated bilayer with $(t_1, t_2) = (0, 1)$ are shown in figures (b) and (d). The flat band is colored blue.

a one dimensional problem, we start with the proof of point (c) of theorem 2 in subsection 4.1. In subsections 4.2 and 4.3 we present procedures for obtaining CSOBs for NN projectors. In subsection 4.4, we discuss how to determine whether a projector is NN-reducible, and show how a supercell representation can be used to extend the results for NN projectors to the more general class of NN-reducible projectors. In subsection 4.5, we discuss the topological properties of SL projectors as well as projectors associated with CSOBs and CS hybrid WFs.

4.1. Hybrid Wannier functions for strictly local projectors

As discussed in the introduction, hybrid WFs are a variant of WFs for $d > 1$ dimensional translationally-invariant systems. Hybrid WFs can be obtained by taking the inverse Fourier

transform of the Bloch wavefunctions along exactly one dimension. Such wavefunctions can be chosen to be localized and Wannier-like along one dimension, and Bloch wave-like and delocalized along the other dimensions. Starting with a real space representation of a TI SL projector, we outline a procedure for obtaining such a basis, so that it is compact localized along the localized dimension. We will use the convention (2) of expressing the Hilbert space as a tensor product, $\mathbb{Z}^{\otimes d} \otimes \mathcal{H}$, throughout this section, where $\mathcal{H}$ represents the space of orbitals and spin.

First, we revisit the k-space, or Fourier space representation for a projector. As is customary, we consider finite periodic lattices of size $L_1 \times \ldots \times L_d$, so that the number of sites $N = L_1 \ldots L_d$. For infinite lattices, we take the limit of the lengths going to infinity. Without loss of generality, we choose the direct lattice to be a hyper-cube so that the Brillouin zone (B.Z.) consists of reciprocal lattice vectors $\vec{k}$ satisfying $\vec{k}.\vec{R} \in 2\pi\mathbb{Z}$ for any $\vec{R} \in \mathbb{Z}^d$ such that $k_i \in (-\pi, \pi]\ \forall i \in \{1, \ldots, d\}$. An orthogonal band projection operator P can be expressed as

$$P = \sum_{\vec{k}\in \text{B.Z.}} |\vec{k}\rangle\langle\vec{k}| \otimes P(\vec{k}),$$

$$\text{where } |\vec{k}\rangle := \frac{1}{\sqrt{N}} \sum_{\vec{r}\in\mathbb{Z}^d} \mathrm{e}^{-\mathrm{i}\vec{k}.\vec{r}} |\vec{r}\rangle,$$

$$\text{and } P(\vec{k}) := \langle\vec{k}|P|\vec{k}\rangle.$$

We have suppressed all orbital quantum numbers in the expressions above to aid readability. Each $P(\vec{k})$ is an $n \times n$ matrix function of $\vec{k}$. Since P is idempotent, $P(\vec{k})P(\vec{k}') = \delta_{\vec{k},\vec{k}'} P(\vec{k})$, i.e. all the $P(\vec{k})$'s for distinct $\vec{k}$'s are mutually orthogonal projection operators.

In order to obtain hybrid WFs which are localized along the mth dimension, we express P in the Fourier space corresponding to all spatial dimensions, except for the mth dimension. Here, we only discuss the case with $m = d$; the rest can be obtained by simple modifications. Let B.Z.$_{d-1}$ denote the B.Z. in $d-1$ dimensions. Denoting the spatial position along the dth dimension by z, we obtain

$$P = \sum_{\vec{k}_\perp \in \text{B.Z.}_{d-1}} |\vec{k}_\perp\rangle\langle\vec{k}_\perp| \otimes P(\vec{k}_\perp), \tag{19}$$

with $\vec{k}_\perp \equiv (k_1, \ldots, k_{d-1})$, and $P(\vec{k}_\perp)$ being an orthogonal projection operator given by

$$P(\vec{k}_\perp) := \sum_{z,z'\in\mathbb{Z}} |z\rangle\langle z'| \otimes \langle\vec{k}_\perp, z|P|\vec{k}_\perp, z'\rangle. \tag{20}$$

Since $P(\vec{k}_\perp)P(\vec{k}'_\perp) = \delta_{\vec{k}_\perp,\vec{k}'_\perp} P(\vec{k}_\perp)$, equation (19) implies that the task of obtaining an orthogonal basis for the image of P can be split into the task of obtaining orthogonal bases for each $P(\vec{k}_\perp)$ individually. Since P is SL, each $P(\vec{k}_\perp)$ can be thought of as being a one dimensional SL projector acting on a lattice with positions $z \in \mathbb{Z}$. Corollary 2 guarantees that each $P(\vec{k}_\perp)$ must have a CS Wannier basis in a size $2b$ supercell representation. This leads us to a procedure of obtaining hybrid WFs which are compact localized along any chosen dimension (see procedure 3).

While in our considerations so far, we have considered an SL projector, if we were to consider a projector which was SL along any one direction without the requirement that it be SL along any of the other directions, it follows from the arguments above that hybrid WFs which

Procedure 3. CS hybrid WFs for SL projectors.

Input: a TI SL projection operator P operating on a d dimensional lattice

Procedure: to obtain hybrid WFs which are Wannier-like along the dth dimension, for every value of $\vec{k}_\perp$ in the $d-1$ dimensional B.Z.:

1. Obtain the $1d$ projector $P(\vec{k}_\perp)$ using expression (20)
2. Use a size b supercell representation to express $P(\vec{k}_\perp)$ as a $1d$ NN projector
3. Following procedure 2, obtain a CW basis for the image of $P(\vec{k}_\perp)$. Let $\tilde{\Pi}_\perp^{\vec{k}_\perp}$ denote this basis
4. Obtain the set $\tilde{\Pi}^{\vec{k}_\perp} \coloneqq \{\vec{k}_\perp \otimes |\psi\rangle : |\psi\rangle \in \tilde{\Pi}_\perp^{\vec{k}_\perp}\}$

Obtain the set

$$\tilde{\Pi} \coloneqq \bigcup_{\vec{k}_\perp}^{B.Z._{d-1}} \tilde{\Pi}^{\vec{k}_\perp}$$

Output: the set $\tilde{\Pi}$ consisting of hybrid WFs within a size $1 \times \ldots \times 1 \times 2b$ supercell representation, which are CS and Wannier-like along the dth dimension

Procedure 4. Construction of a CSOB for any NN projector in arbitrary dimensions.

Input: a NN projector P acting on a $d \geqslant 1$ dimensional lattice
Procedure: divide the lattice into two sets A and B consisting of alternating cells, according to (21)
1. Obtain $\tilde{\Pi}^{P}_{\vec{r}}$ and hence $P_{\vec{r}}$, for every $\vec{r} \in A$
2. Obtain the orthogonal projector $P - P_A \coloneqq P - \sum_{\vec{r}\in A} P_{\vec{r}}$
3. Obtain $\tilde{\Pi}^{P-P_A}_{\vec{r}}$ for every $\vec{r} \in B$

Output: the set $\tilde{\Pi} \coloneqq \left(\bigcup_{\vec{r}\in A} \tilde{\Pi}^{P}_{\vec{r}}\right) \cup \left(\bigcup_{\vec{r}\in B} \tilde{\Pi}^{P-P_A}_{\vec{r}}\right)$ which is a CSOB spanning the image of P

are localized in one direction can still be constructed. This completes our proof for point (c) of theorem 2.

4.2. Nearest neighbor projectors

We now construct a CSOB for nearest-neighbour projectors in d dimensions. Similar to the $1d$ case, the Gram–Schmidt orthogonalization must be carried out in a sequence which guarantees that after any step, the reduced projector remains NN hopping or on-site hopping, if the original projector is NN hopping. We observe that unlike in the $1d$ case, this puts restrictions on the orthogonalization sequence in higher dimensions. Although there are multiple possible types of sequences which ensure this condition is satisfied, for concreteness, here, we present a specific one (in procedure 4), which also be used to obtain a CW basis for TI NN projectors as well.

This procedure relies on dividing the lattice into two sets, A and B consisting of alternating cells similar to what was done in section 3.2. For concreteness, we choose A and B to be given by

$$\begin{aligned} A &= \left\{ \vec{r} : \vec{r} \in \mathbb{Z}^d; \sum_{i=1}^{d} r_i \in 2\mathbb{Z} \right\}; \\ B &= \left\{ \vec{r} : \vec{r} \in \mathbb{Z}^d; \sum_{i=1}^{d} r_i \in 2\mathbb{Z}+1 \right\}. \end{aligned} \tag{21}$$

Since any two distinct cells $\vec{r}_1, \vec{r}_2 \in A$ are separated by at least two hops, $P_{\vec{r}_1} P_{\vec{r}_2} = 0$, and hence $P_A \coloneqq \sum_{\vec{r}\in A} P_{\vec{r}}$ is an orthogonal projector.

Lemma 4. *The orthogonal projector $P - P_A$ satisfies $\langle \vec{r}_1, i|(P-P_A)|\vec{r}_2, j\rangle = 0$ for all $i, j \in \{1, \ldots, n\}$, unless $\vec{r}_1 = \vec{r}_2 \in B$.*

Proof. Let $\hat{\delta}_i$ denote the unit vector along dimension i. Similar to the proof for $1d$ projectors (lemma 1), we introduce the diagonal basis (cf (11)), with the primes dropped for notational convenience. As before, we denote the diagonal of the $P_{\vec{r}\vec{r}}$ matrix in this representation by $d_{\vec{r}}$, so that $\langle \vec{r}, \alpha|P|\vec{r}, \beta\rangle = (d_{\vec{r}})_\beta \delta_{\alpha\beta}$.

Since $P|\vec{r}, \alpha\rangle = P_A|\vec{r}, \alpha\rangle$ whenever $\vec{r} \in A$, both $\vec{r}_1$ and $\vec{r}_2$ must belong to B for the corresponding matrix element to be non-zero. If $\vec{r}_1, \vec{r}_2 \in B$ and are distinct, we get

$$\begin{aligned} \langle \vec{r}_1, \alpha|P - P_A|\vec{r}_2, \beta\rangle &= -\langle \vec{r}_1, \alpha|P_A|\vec{r}_2, \beta\rangle \\ &= -\langle \vec{r}_1, \alpha| \sum_{s=\pm 1} \sum_{m=1}^{d} P_{\vec{r}_2 + s\hat{\delta}_m} |\vec{r}_2, \beta\rangle, \end{aligned} \tag{22}$$

since $P_{\vec{r}}|\vec{r}_2, \beta\rangle = 0$ unless $\vec{r}$ is a nearest neighbor of $\vec{r}_2$. Since P only has NN hopping terms, this is zero, unless $\vec{r}_1$ and $\vec{r}_2$ are equal to each other, or are two hops away from each other,

i.e. only if $\vec{r}_2$ is of the form $\vec{r}_1 \pm \hat{\delta}_p \pm \hat{\delta}_q$ for some $p, q \in \{1, \ldots, d\}$. In order to show that the matrix element is zero for the case with two hops, we will require the higher dimensional analogs of equations (12)–(14), which are

$$\langle \vec{r}, \alpha | P | \vec{r}, \alpha \rangle \geqslant 0, \tag{23}$$

$$\langle \vec{r}, \alpha | P | \vec{r}, \alpha \rangle + \langle \vec{r} + \hat{\delta}_p, \beta | P | \vec{r} + \hat{\delta}_p, \beta \rangle = 1 \quad \forall\ p \in \{1, \ldots, n\},$$

$$\text{whenever } \langle \vec{r}, \alpha | P | \vec{r} + \hat{\delta}_p, \beta \rangle \neq 0, \tag{24}$$

$$\text{and} \sum_{\gamma} \sum_{\vec{v}}^{\text{c.n.}} \langle \vec{r}, \alpha | P | \vec{v}, \gamma \rangle \langle \vec{v}, \gamma | P | \vec{w}, \beta \rangle = 0 \tag{25}$$

respectively. The summation in (25), with a superscript 'c.n.' (for common neighbors) is over those vectors $\vec{v}$ which are NNs of both $\vec{r}$ and $\vec{w}$.

For the case where $\vec{r}_2$ is two hops away from $\vec{r}_1$, expression (22) simplifies to zero as follows:

$$\begin{aligned} \langle \vec{r}_1, \alpha | \sum_{m=1}^{d} P_{\vec{r}_2 + \hat{\delta}_m} | \vec{r}_2, \beta \rangle &= \langle \vec{r}_1, \alpha | \sum_{\vec{w}}^{\text{c.n.}} P_{\vec{w}} | \vec{r}_2, \beta \rangle \\ &= \sum_{\vec{w}}^{\text{c.n.}} \sum_{\gamma}^{(d_{\vec{w}})_\gamma \neq 0} \frac{\langle \vec{r}_1, \alpha | P | \vec{w}, \gamma \rangle \langle \vec{w}, \gamma | P | \vec{r}_2, \beta \rangle}{\langle \vec{w}, \vec{\gamma} | P | \vec{w}, \gamma \rangle}. \end{aligned}$$

If $\langle \vec{r}_1, \alpha | P | \vec{r}_1, \alpha \rangle = 1$, then every term in the summation is zero. Otherwise, we get

$$\begin{aligned} \ldots &= \frac{(\delta_{\vec{r}_1})_\alpha}{1 - \langle \vec{r}_1, \alpha | P | \vec{r}_1, \alpha \rangle} \sum_{\vec{w}}^{\text{c.n.}} \sum_{\gamma} \langle \vec{r}_1, \alpha | P | \vec{w}, \gamma \rangle \langle \vec{w}, \gamma | P | \vec{r}_2, \beta \rangle \quad \text{from (24)}, \\ &= 0, \qquad \text{from (25)}. \end{aligned}$$

Thus, matrix elements of $P - P_A$ can be non-vanishing only if $\vec{r}_1 = \vec{r}_2 \in B$. □

The basis vectors obtained using procedure 4 consist of wavefunctions which have a maximum spatial extent (volume) of at most $3 \times \ldots \times 3$ cells. As shown in figure 11, they are in fact significantly smaller in extent than this upper bound.

4.3. Translationally invariant nearest neighbor projectors

Let $\widehat{\mathcal{T}}_i$ denote the unit translation operator along the ith dimension. For $\vec{r} \in \mathbb{Z}^d$, let $\widehat{\mathcal{T}}_{\vec{r}}$ denote a translation by an amount $\vec{r}$.

Although procedure 4 can also be used to generate a CS orthonormal basis from TI projectors, in general the resulting basis will not be a Wannier basis. However, the wavefunctions can be chosen to have translational invariance properties if each $\tilde{\Pi}^{P}_{\vec{r}}$ ($\tilde{\Pi}^{P-P_A}_{\vec{r}}$) for $\vec{r} \in A$ ($\vec{r} \in B$) is chosen to be a translation of $\tilde{\Pi}^{P}_{\vec{0}}$ ($\tilde{\Pi}^{P-P_A}_{\hat{\delta}_1}$) by $\vec{r}$ ($\vec{r} - \hat{\delta}_1$) cells. Based on this principle, we propose a method (procedure 5) for obtaining a CS Wannier basis spanning the image of P within a supercell representation. For $d = 1$, this procedure is equivalent to procedure 2.

Using steps similar to those used for proving theorem 3, we can show that procedure 5 outputs a CW basis as claimed.

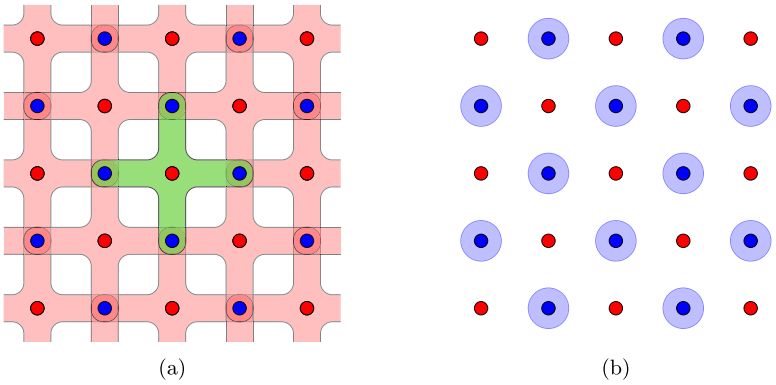

(a) (b)

Figure 11. Procedure 4 for a $2d$ NN *projector*: cells belonging to sets A and B are represented by red and blue dots respectively. (a) In order to obtain P_A, we operate P on each cell belonging to A, and orthogonalize the vectors. Each colored shape centered at location $\vec{r}$ denotes the maximum spatial extent of the wavefunctions in $\tilde{\Pi}^P_{\vec{r}}$. (We show one shape in green, in order to highlight the 'plus' shape of each of these sets). (b) Since $P - P_A$ is on-site hopping, operating it on any cell in set B creates wavefunctions which are localized at exactly that cell. Each blue circle centered at $\vec{r} \in B$ represents the maximum extent of vectors in $\tilde{\Pi}^{P-P_A}_{\vec{r}}$.

Procedure 5. CS Wannier basis for d dimensional NN projectors.

Input: a TI NN projection operator P on a d dimensional lattice
Procedure:

1. Obtain Π^P_0, and orthogonalize it to obtain the set $\tilde{\Pi}^P_0$
2. Obtain the orthogonal projection operator P_0 onto the span of Π^P_0
3. Obtain a reduced projection operator (which removes all the NNs of the site $\hat{\delta}_1$)
$$P' \coloneqq P - \sum_{i=1}^{d} \widehat{\mathcal{T}}_i \widehat{\mathcal{T}}_1 P_0 \widehat{\mathcal{T}}_1^\dagger \widehat{\mathcal{T}}_i^\dagger - \sum_{i=1}^{d} \widehat{\mathcal{T}}_i^\dagger \widehat{\mathcal{T}}_1 P_0 \widehat{\mathcal{T}}_1^\dagger \widehat{\mathcal{T}}_i$$
4. Obtain and orthogonalize $\Pi^{P'}_{\hat{\delta}_1}$ to obtain the set $\tilde{\Pi}^{P'}_{\hat{\delta}_1}$
5. Obtain the set Π, defined as
$$\Pi = \left(\bigcup_{\vec{r} \in A} \{ \widehat{\mathcal{T}}_{\vec{r}} |\chi\rangle : |\chi\rangle \in \tilde{\Pi}^P_0 \} \right) \cup \left(\bigcup_{\vec{r} \in B} \{ \widehat{\mathcal{T}}_{\vec{r} - \hat{\delta}_1} |\chi\rangle : |\chi\rangle \in \tilde{\Pi}^{P'}_{\hat{\delta}_1} \} \right) \tag{26}$$

Output: the set Π consisting of CS WFs spanning the image of P, within a size $2 \times \ldots \times 2$ supercell representation

4.4. Supercell representation and nearest neighbor reducible projectors

We now discuss how to extend the results and methods for NN projectors to SL projectors with larger hopping distances. To that end, we use a supercell representation analogous to the one used for $1d$ in section 3.3. Unlike in $1d$ where every SL projector is an NN projector in some supercell representation, in general, an SL projector in $d > 1$ becomes a *next*-nearest-neighbor (NNN) hopping projector instead of an NN projector using this transformation. Specifically, if the maximum hopping distance of an SL projector is b, then the projector has at most NNN hopping terms within a size $b \times \ldots \times b$ supercell representation (see figure 12). This reversible transformation is associated with the correspondence:

Primitive cell representation $\longleftrightarrow$ Supercell representation

$$|r_1, \ldots, r_d, i\rangle \equiv \left| r_1 \backslash b, \ldots, r_d \backslash b, i + \sum_{m=1}^{d} n^m (r_m \bmod b) \right\rangle_s, \tag{27}$$

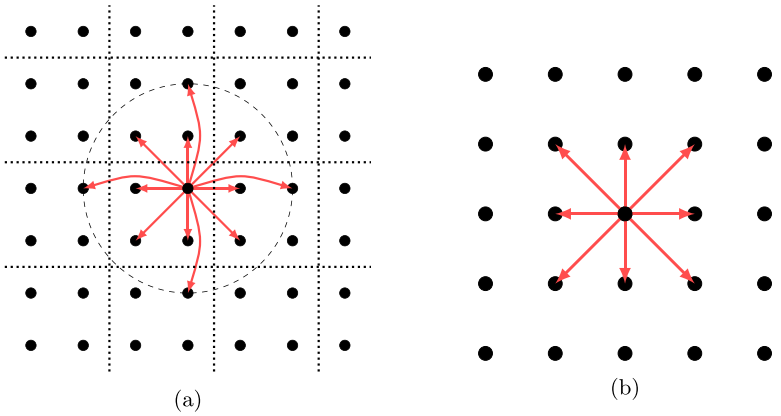

Figure 12. Each black dot represents a lattice cell (which may consist of multiple orbitals). The dashed circle denotes the maximum hopping distance from that cell. (a) The connectivity of a generic SL operator with a maximum hopping distance of $b = 2$. Hopping elements from an arbitrary cell are shown in red. Grouping all the sites within each cell of a 2×2 grid, we obtain a supercell representation. (b) The operator becomes an NNN hopping operator in the supercell representation. Here, the operator connects neighboring cell along the $\hat{x}$, $\hat{y}$, as well as the $\hat{x} \pm \hat{y}$ directions, with $\hat{x}$ and $\hat{y}$ denoting the two axes.

Since the methods developed in sections 4.2 and 4.3 are applicable only to NN projectors (and not general NNN projectors), even after using a supercell representation, these techniques cannot be applied to a general SL projector operator for $d > 1$.

Hence, we look for projectors that have an NN-hopping form using suitable transformations. We call such projectors NN-reducible. Which SL projectors are NN-reducible? While SL projectors with various types of connectivity are NN-reducible, here we highlight some particularly simple cases. It is easy to see that SL projectors that satisfy $\langle \vec{r}, i|P|\vec{r}\,', j\rangle = 0$, whenever $\vec{r} - \vec{r}\,'$ is not along any of the primitive cell directions become NN hopping within a supercell representation of the type described above. For example, an SL projector on a square lattice that has non-zero hoppings only along the $\pm\hat{x}$ and $\pm\hat{y}$ directions, but no other direction is NN-reducible. This is in contrast with the NNN-reducible projectors of the type shown in figure 12(b). For some SL projector that appear to be of an NNN form after the transformation (27), it may still be possible to apply the results from the previous sections to obtain CS WFs. For example, if an SL projector on a square lattice in a supercell representation only connects neighboring cells along the $\hat{x}$ and $\hat{x} + \hat{y}$ directions, the projector is NN-hopping if we regard these two vectors as being the lattice vectors. We consider all such SL projectors that can be brought to an NN form using change of primitive cell vectors and supercell transformations as NN-reducible. Without loss of generality, we only consider NN-reducible projectors that have hopping elements only along the primitive cell directions below.

For such projectors, we obtain the following results:

Corollary 3. *If an SL projector with a maximum hopping distance b is NN reducible, its image is spanned by a CSOB consisting of wavefunctions of a maximum spatial extent of* $3b \times \ldots \times 3b$ *cells.*

The procedure for obtaining such a basis is summarized in the following table:

Primitive cell representation	$\xrightarrow[b\times\ldots\times b]{\text{Size}}$	Supercell representation		$\to$ Primitive cell representation
SL projector ($b \geqslant 1$)	$\to$	NN projector ($b = 1$)	$\xrightarrow{\text{Procedure 4}}$	CSOB (max size 3) $\to$ CSOB (max size $3b$)

Corollary 4. *If a TI SL projector with a maximum hopping distance b is NN reducible, its image is spanned by a CS Wannier basis within a size* $2b \times \ldots \times 2b$ *supercell representation.*

The procedure for obtaining such a basis is summarized in the following table:

Primitive cell representation	$\xrightarrow{\text{Size } b}$	Size b supercell representation	$\xrightarrow{\text{Size 2}}$	Size $2b$ supercell representation
SL projector ($b \geqslant 1$)	$\to$	NN projector ($b = 1$)	$\xrightarrow{\text{Procedure 5}}$	CS Wannier basis

This completes our proof for theorem 2.

4.5. Topological triviality and compact bases

So far, we have investigated the conditions under which is it possible for a band to be spanned by compactly supported orthogonal bases (CSOBs) or by CS hybrid WFs. Specifically, we identified localization properties of associated projection operators that are necessary or sufficient for the existence of such bases. Similar questions regarding the existence of localized WFs have a long history, as noted in the introduction. The existence of exponentially localized WFs has a bearing on the topological properties of the corresponding bands, with non-trivial band topology restricting the degree of localization possible for WFs. This motivates us to investigate the topological properties of bands possessing CSOBs.

We start with a brief overview of known results. Thouless [36] showed that well localized magnetic WFs can be constructed in $2d$ if and only if the Chern number is zero. For $d \leqslant 3$, it was later shown that in the presence of time-reversal symmetry and translational invariance, exponentially localized WFs corresponding to an isolated band or a set of isolated bands always exist [7, 9, 10, 56]. For systems with other symmetry properties, the existence of such localized WFs is not guaranteed, or even impossible, when the bands are topologically non-trivial. For instance, bands with non-zero Chern numbers do not possess exponentially localized WFs [57]. More generally, there exists a *localization dichotomy* [37] which says that either exponentially localized WFs exist and the Chern numbers are zero, or all WFs are delocalized (with diverging second moment of the position operator) and the Chern numbers are non-zero. Recently, this result was partially extended to disordered systems [58], with a proof for the vanishing of the Chern marker for $2d$ insulators possessing exponentially localized generalized WFs.

Since CS WFs (in R^n) are even more localized than generic exponentially local WFs, one may expect topological triviality to follow immediately from these results. While we find this to be true (as discussed below), care is needed while drawing such a conclusion. In all the works discussed above, the wavefunction localization is described in terms of decay of wavefunction amplitude in real space, i.e. R^n. We note that this notion of localization may not in general be the same as localization in tight-binding models which we consider in this paper. Specifically, orbitals on the lattice ($\mathbb{Z}^n$) which are used as the basis in tightbinding descriptions may themselves not be CS, or even exponentially localized in space (R^n). Thus the wavefunctions which are linear combinations of a finite set of such tightbinding orbitals do not in general vanish outside a certain bounded region in space as one might otherwise assume from the use of the term 'compact support' in describing these wavefunctions.

A number of results relating compact support localization of WFs in tight-binding models and topological triviality of associated bands are relevant to the cases considered in this paper. Specifically, it was proved that flat bands in $2d$ flat-bands Hamiltonians that are SL in a tight-binding sense always have a Chern number of zero [21]. This property can be viewed as arising due to the fact that the flat bands in such models are spanned by CS Wannier-type functions or CLSs. More recently, this result was generalized to all symmetry classes and arbitrary dimensions greater than one, by proving that the vector bundle associated with band(s) that are spanned by CS Wannier-type functions are topologically trivial [20]. As discussed in section 2.2, CS Wannier-type functions are in general non-orthogonal, and consequently the orthogonal WFs we consider in this paper are a special type of CS Wannier-type functions. Similarly, the set of SL projectors is a subset of the set of projectors that have their images spanned by CS Wannier-type functions. Thus, it follows directly from the results in [20] that:

Theorem 3. *For TI tight-binding models in $d > 1$, a set of bands that is spanned by CS WFs is topologically trivial. More generally, bands associated with SL projectors are topologically trivial.*

It follows that TI NN and NN-reducible projectors are topologically trivial, since they are SL.

While a topological obstruction exists for constructing localized WFs, no such obstruction exists for localized hybrid WFs. Since hybrid WFs can be treated as $1d$ WFs (see section 4.1), using the arguments in [11], it follows that for any number of dimensions, hybrid WFs that are exponentially localized along the localized axis exist, independent of the topological properties of the associated band(s). For example, as can be seen using the Coulomb gauge, quantum Hall systems admit localized hybrid Wannier-like solutions that are exponentially decaying along one direction, despite the Chern number being non-zero [59]. Similarly, anomalous quantum Hall systems possess maximally localized hybrid WFs that are exponentially localized [40] despite a non-vanishing Chern number. These statements do no preclude the possibility of a topologically non-trivial band being spanned by CS hybrid Wannier functions. An interesting consequence of the theorem above, and the equivalence of strict localization of a projector, and the existence of CS hybrid WFs along all axes, we find that such bands are *necessarily* topologically trivial. Specifically:

Theorem 4. *For a $d > 1$ dimensional system, if a set of bands is such that for any of the* d *orthogonal axes, there exist hybrid WFs (spanning the bands) that are CS along the chosen axis, then the band(s) are topologically trivial.*

In this section, we have so far only considered systems which are TI. It would be interesting to study the topological properties of similar systems without translational invariance. For example, an analog of CS hybrid WFs could be a set of wavefunctions not related by lattice translations that are each CS along one direction, but possibly delocalized along the other directions. We leave the question of topological triviality of such cases for future work.

Based on physical ground we anticipate that even non-TI SL projectors as well as bands associated with CSOBs should be topologically trivial. Using simple arguments applied to recent results from the literature, we will now show that the latter statement is indeed true. Specifically, we consider projectors that have no symmetries except possibly lattice translation symmetry, i.e. class A systems from the Altland–Zirnbauer classification scheme [60]. The topological classification of systems across all dimensions is organized in the form of a periodic table [61, 62]. As can be seen from the table, odd dimensional class A projectors are always K-theoretically trivial. However, in $2n$ dimensions, they are characterized by the integer valued nth Chern number [63].

Using simple arguments, we will now show that the topological Chern invariant for class A projectors that are associated with CSOBs is zero.

Theorem 5. *In all dimensions, if a projector without symmetries* (*except possibly lattice translation symmetry*) *is such that its image is spanned by a CS orthogonal basis, then it is Chern trivial.*

We only need to show that such projectors in even dimensions are Chern trivial. To that end, we use the real space expression from [63], for the integer valued Chern number, which for a $2n$ dimensional system is given by

$$\mathrm{Ind}\, P = -\frac{(2\pi \mathrm{i})^n}{n!}\sum_{\sigma}(-1)^{\sigma}\ \mathrm{Tr}\ P[\theta_{\sigma_1}, P]\ldots[\theta_{\sigma_n}, P], \tag{28}$$

where Tr denotes the trace operation, the summation is over all permutations σ, and θ_i denotes the projection operator onto the positive half plane along the ith direction, i.e. $\theta_i = \sum_{\alpha}\sum_{r_i>0}|\vec{r},\alpha\rangle\langle\vec{r},\alpha|$. Our arguments are based on the following properties of the index: (i) the additivity of the index for mutually orthogonal projectors, (ii) the independence of the index from the choice of the origin, or axes, and (iii) the local computability of the index. Physically, since the $2d$ case is of the most interest, we demonstrate our arguments by applying them to the $2d$ case. These arguments and the conclusion are valid for higher dimensional cases as well.

First, we note that for $2d$, the index is the same as the Chern marker expression [64, 65], which is the real space analog of the k-space expression for Chern number used for periodic systems. The Chern marker for a projector P is given by

$$\mathrm{Ch}\, P = -2\pi\mathrm{i}\ \mathrm{Tr}\ P[[\theta_x, P], [\theta_y, P]]. \tag{29}$$

As shown explicitly in [64], the Chern marker is additive, i.e. Chern marker of the sum of two mutually orthogonal projectors is the sum of the Chern markers of the two projectors.

Consider a CSOB of size R, consisting of wavefunctions $|\psi_i\rangle$. Let P be the orthogonal projector onto the span of the CSOB. Clearly, P is SL, and is the sum of the orthogonal projection operators P_i projecting onto states $|\psi\rangle_i$'s:

$$\begin{aligned} P &= \sum_{i=1} P_i; \\ \text{with } P_i &= |\psi_i\rangle\langle\psi_i|, \\ P_i P_j &= \delta_{ij} P_i. \end{aligned} \tag{30}$$

By definition, each wavefunction $|\psi_i\rangle$ has non-zero support only within a circle B_i centered at some location $\vec{c}_i$ of radius R. (The $\vec{c}_i$'s are not unique; however, the conclusions that follow do not depend on the choice.) Thus, each projector P_i has non-zero hopping terms only within B_i.

From (29), we note that $\mathrm{Ch}\, P_i \neq 0$ only if $|\psi_i\rangle$ straddles both the axes, i.e. if $|\vec{c}_i| \leqslant R$, and is zero otherwise. For example, if B_i lies entirely in the right half plane, then the operator θ_x can be replaced by the identity operator in equation (29), resulting in a zero Chern marker (and similarly for other cases). Using this, and the additivity of the Chern marker, we obtain

$$\mathrm{Ch}\, P = \mathrm{Ch}\underbrace{\left(\sum_{|\vec{c}_i|\leqslant R} P_i\right)}_{\tilde{P}} + \mathrm{Ch}\left(\sum_{|\vec{c}_i|>R} P_i\right) = \mathrm{Ch}\,\tilde{P}.$$

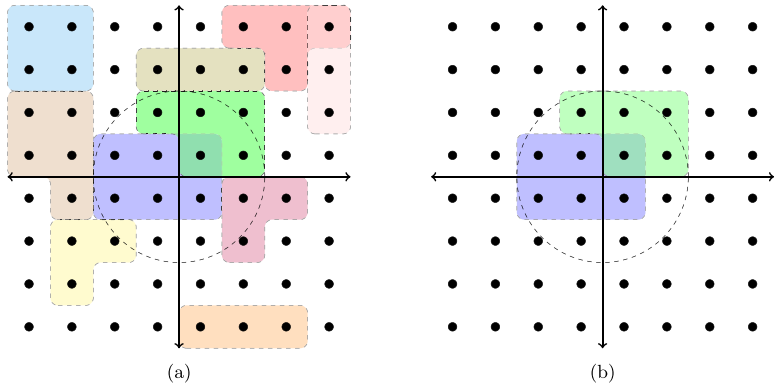

Figure 13. An illustrative example in $2d$. (a) Each basis state $|\psi_i\rangle$ of a CSOB of size $R = 2$ is shown by a colored region, and has non-zero support only on the sites within that region. (b) Only those wavefunctions that have their centers $\vec{c}_i$'s inside the dashed circle have non-zero contributions to the Chern marker. Retaining only these wavefunctions defines a new projector $\tilde{P}$, which has the same Chern number as P.

(For a cartoon picture see figure 13.) Since the Chern number is independent of the choice of the origin, we may shift the origin and reevaluate the Chern number without affecting its value. Consider moving the origin by a distance of at least $2R$ in any direction. For example, let the new location of the origin be $(-3R, -3R)$. Since none of the constituent wavefunctions of $\tilde{P}$ straddle both of the new axes, $\mathrm{Ch}\,\tilde{P} = 0$. Consequently,

$$\mathrm{Ch}\,P = 0.$$

The Chern marker is additive in all dimensions. Thus, applying the same reasoning to equation (28), it is easy to show that projectors associated with CSOBs are Chern trivial in all dimensions.

5. Conclusions

In this paper, we have obtained necessary and sufficient conditions for a band or a set of bands to be spanned by compactly supported Wannier functions, or in the absence of lattice translational invariance, for a subspace of the Hilbert space to possess an orthogonal basis consisting of compactly supported wavefunctions. In $1d$ tight-binding models, we have established that there exists a compactly supported orthogonal basis spanning the occupied subspace iff the corresponding projection operator is Strictly local. In the process, we presented an algorithm for constructing a compactly supported orthogonal basis for the image of any Strictly local projector. This algorithm generates wavefunctions having a maximum spatial extent three times the maximum hopping distance of the projector. Nearest neighbor projectors on a Bethe lattice with arbitrary coordination number also have a compactly supported orthonormal basis. In the appendix A, a simple method for the construction of some Strictly local projectors is provided.

For higher dimensional lattices, we showed that while strict locality of the projector is a necessary condition for the existence of a compactly supported orthogonal basis, a sufficient condition is that the projector be expressible as a nearest neighbor projector using a change of primitive cell vectors or a supercell representation. For such projectors, which we call nearest neighbor reducible, we presented an algorithm for constructing a compactly supported orthogonal basis, or a compactly supported Wannier basis when TI. Additionally, we showed hybrid

Wannier functions that are compactly supported can be constructed for any choice of the localization axis iff the associated projector is Strictly local. Since the localization properties of band projectors and Wannier functions are closely related to band topology, we also showed that all TI Strictly local projectors in systems with dimensions two and higher are topologically trivial. Additionally, using some simple arguments, we have shown that projectors without any symmetry other than possibly lattice translation symmetry, that are associated with compactly supported orthogonal bases are Chern trivial. Moreover, the existence of hybrid Wannier functions that are compactly supported along the localized axis for any choice of the localized axis implies topological triviality, unlike exponentially localized hybrid Wannier functions, which can exist even for topologically non-trivial bands.

Our results suggest a number of interesting directions for future work. The compactly supported orthogonal bases resulting from our construction may not be maximally localized. It would be interesting to improve the bounds on the spatial support of these basis functions, and also formulate an analytic procedure which results in maximally localized orthogonal basis functions. In the case of TI projectors, our procedures generate Wannier bases in supercell representations. A natural follow-up would be to find minimal sized supercell representations which have compactly supported Wannier bases. Here, we have shown that a Strictly local projector and a compact orthonormal basis are essentially equivalent on $1d$ lattices. For dimensions two and higher, it would be useful to identify locality conditions on the projector operator that are equivalent to the existence of a compactly supported orthogonal basis. It would also be interesting to prove or disprove the topological triviality of Strictly local projectors in arbitrary dimensional systems in the absence of lattice translational invariance.

Acknowledgments

We thank A Culver, D Reiss, X Liu, A Brown and L Lindwasser for useful discussions and comments. PS, FH and RR acknowledge support from the NSF under CAREER Grant No. DMR-1455368, and from the Mani L Bhaumik Institute for Theoretical Physics. PS and RR acknowledge the funding support from the University of California Laboratory Fees Research Program funded by the UC Office of the President (UCOP), Grant ID LFR-20-653926.

Data availability statement

No new data were created or analysed in this study.

Appendix A

A.1. compactly supported Wannier functions for an example Hamiltonian

In this section, we discuss an example of an Strictly local projector in $1d$, and compare our results with numerical techniques from the literature. To our knowledge, there are no simple methods in the literature of proving that the span of generic Strictly local projectors possess a CSOB. Here, we consider the following example of a $1d$ two-band (TI) Hamiltonian given in k-space by

$$H(k) = \frac{1}{6}\begin{pmatrix} 3\sin k + \cos k\left(2\sqrt{2}\cos k - 2\sqrt{2}\sin k + 8\sqrt{2} + 3\right) & (\cos k - \sin k + 4)\left(\mathrm{i} - 2\sqrt{2}\sin k\right) \\ -(\cos k - \sin k + 4)(\mathrm{i} + 2\sqrt{2}\sin k) & (\cos k + 2)(3 - 2\sqrt{2}\cos k) + (2\cos k\sqrt{2} + 3)(\sin k - 2) \end{pmatrix}. \tag{31}$$

The two energy bands of this Hamiltonian are $E_1(k) = 2 + \cos k$, and $E_2(k) = -2 + \sin k$. The band projector corresponding to the E_1 band is given by

$$P(k) = \frac{1}{6}\begin{pmatrix} 2\cos(k)\sqrt{2}+3 & \mathrm{i} - 2\sqrt{2}\sin(k) \\ -\mathrm{i} - 2\sqrt{2}\sin(k) & 3 - 2\sqrt{2}\cos(k) \end{pmatrix}, \tag{32}$$

which is an Strictly local projector. Since the projector is TI, we seek a Wannier basis. Our theorem implies that there exist compactly supported Wannier functions spanning each of the two bands in a size-two supercell representation.

Usually, Wannier functions are computed by first obtaining the corresponding Bloch wavefunctions. For the example projector, the Bloch wavefunction (up to a phase) is

$$\psi_1(k) = \frac{1}{\sqrt{6}}\begin{pmatrix} \dfrac{2\sqrt{2}\sin(k) - \mathrm{i}}{\sqrt{3 - 2\sqrt{2}\cos(k)}} \\ -\sqrt{3 - 2\sqrt{2}\cos(k)} \end{pmatrix}. \tag{33}$$

A corresponding Wannier basis is then obtained through a Fourier transform of the Bloch wavefunction. Specifically, a Wannier function $w_1^R(z)$ localized at cell R can be obtained using

$$w_1^R(z) = \frac{L}{2\pi}\int_{-\pi}^{\pi} \mathrm{d}k\, \mathrm{e}^{\mathrm{i}k(R-z)}\psi_1(k), \tag{34}$$

where L is the system size. Since $\psi_1(k)$ is a smooth function of k, the corresponding Wannier function is exponentially localized (see figure 14). However, Wannier functions are not unique, because of a gauge degree of freedom:

$$\psi_1(k) \to \mathrm{e}^{\mathrm{i}\theta(k)}\,\psi_1(k).$$

A more localized Wannier basis can be obtained by using a 'better' gauge $\theta(k)$.

While it is not the objective of this paper to obtain maximally localized Wannier functions (MLWFs) for Strictly local projectors, it is useful to compare our approach with the MLWF procedure [11]. The k-space MLWF procedure converges to the optimal gauge using a gradient descent procedure on an initial 'guess' Wannier basis. While our numerical experiments indicate that the MLWF procedure generates compactly supported Wannier functions (which are usually different from the ones obtained using procedure 2), they do not guarantee the existence of compactly supported Wannier functions for arbitrary Strictly local projectors. In contrast, our procedure is analytical, and generates wavefunctions that are exactly CS.

For non-TI projectors, a notable point of similarity between the MLWF procedure and our approach is the starting point which involves choosing 'trial orbitals' on which the projector is operated. In both procedures, the post-projection wavefunctions are orthonormalized (followed by gradient descent in the case of the MLWF algorithm). While the MLWF procedure uses the Lowdin (i.e. symmetric) orthogonalization procedure [50], we use the Gram–Schmidt procedure. This is intentional: the Lowdin procedure is applicable only if the set to be orthogonalized is linearly independent, while the Gram–Schmidt procedure lacks this restriction. Hence, for generic Strictly local projectors, the real space MLWF procedure requires suitably chosen trial orbitals. While such a choice may exist, we are not aware of a general method for obtaining one for arbitrary Strictly local projectors. A much simpler approach (which we adopt) is to choose all the orbitals $|\vec{r}, n\rangle$ as trial orbitals. The set $\Pi_{\vec{r}}^P$ (defined in (3)) which is generally linearly dependent can then be orthonormalized using the Gram–Schmidt procedure.

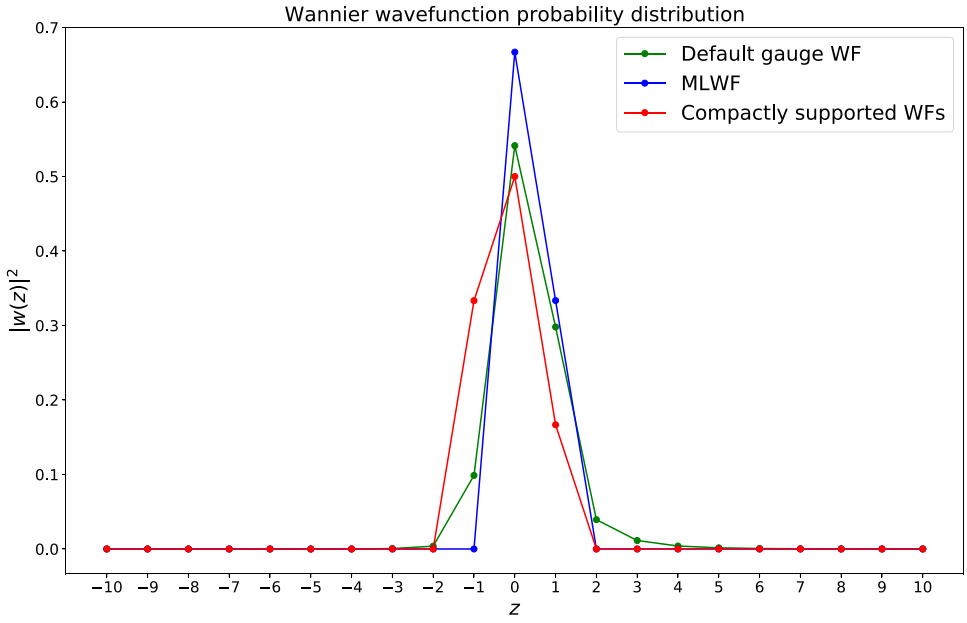

Figure 14. WFs centered at $R = 0$, corresponding to three different gauge choices and corresponding to the span of (32) are shown. The wavefunction probability is plotted a function of position. Green: numerically obtained Wannier function corresponding to (33) is exponentially localized. Blue: numerically obtained MLWF is CS up to numerical precision. Red: the two CS WFs obtained analytically using procedure 2 in a size 2 supercell representation have the same probability distribution in the primitive cell representation.

A.2. A simple method for constructing Strictly local projectors

In this section, we present a simple method for constructing TI Strictly local projectors in one and two dimensions. We note that while one may use the equivalence that we have proven for $1d$ and construct Strictly local projectors from a compactly supported TI orthogonal basis, such a method is not entirely straightforward to implement since one first needs to construct a TI orthogonal basis which is compactly supported and of an appropriate size. A much simpler alternative inspired by Clifford algebras can however be used, wherein an nearest neighbor projector can be constructed by first obtaining what we call an nearest neighbor *flat* Hamiltonian. Such a flat Hamiltonian is an example of a flat-band Hamiltonian with all bands being flat and with energies ± 1. We obtain the projector P onto the -1 eigenspace of H, and note that the since $H = \mathbb{1} - 2P$, P is guaranteed to be a nearest neighbor projector. We start by constructing an example of a $1d$ nearest neighbor flat-band Hamiltonian in appendix A.2.1, followed by a construction of a $2d$ nearest neighbor flat band Hamiltonian in appendix A.2.2. While we explicitly describe the procedure only for Strictly local projectors in 1 and 2 dimensional lattices, this method can be straightforwardly generalized to higher dimensions, and larger hopping distances. Although there exist Strictly local projectors that cannot be generated using this method, it can still be used to create many interesting examples of Strictly local projectors.

*A.2.1. 1*d *strictly local projectors.* It is convenient to utilize the Fourier space representation since we only consider TI projectors. First, we construct a flat nearest neighbor Hamiltonian H, from which we will extract the desired nearest neighbor projector. For H to be an nearest

neighbor Hamiltonian, its Fourier space representation must be of the form:

$$H(k) = C_+ \, \mathrm{e}^{\mathrm{i}k} + C_0 + C_- \, \mathrm{e}^{-\mathrm{i}k},$$

with C_+, C_- and C_0 being $n \times n$ matrices which are constrained by the equations $H(k)^\dagger = H(k)$, and $H(k)^2 = 1$. For simplicity, we choose H to possesses two bands. Consequently, $H(k)$ can be expressed in terms of the identity matrix $1_{2\times 2}$ and the two-dimensional Pauli matrices $\{\sigma_i\}$ as

$$H(k) = a_0(k) 1_{2\times 2} + \sum_{i=1}^{3} a_i(k)\sigma_i.$$

Since $\{\sigma_i, \sigma_j\} = 2\delta_{ij}$, the condition that $H(k)$ is flat translates to $\sum_{\mu=0}^{3} a_\mu^2(k) = 1$ and $a_i a_0 = 0$. In order to obtain interesting solutions, we choose $a_0 = 0$. Together with $H^\dagger = H$, this implies that

$$\begin{aligned} a_1(k)^2 + a_2(k)^2 + a_3(k)^2 &= 1; \\ a_i(k)^* &= a_i(k). \end{aligned} \tag{35}$$

Since the Hamiltonian is of an nearest neighbor form, each $a_i(k)$ is expressible as

$$a_i(k) = c_i X + c_i^* X^{-1} + d_i,$$

with complex c_i's, real d_i's, and $X := \mathrm{e}^{\mathrm{i}k}$. Conditions (35) imply that

$$\begin{aligned} \sum_i c_i^2 &= 0 \\ \sum_i c_i d_i &= 0 \\ \sum_i 2|c_i|^2 + d_i^2 &= 1. \end{aligned} \tag{36}$$

Solutions to these equations can be used to construct various flat Hamiltonians and projectors. A trivial example is one with $c_i = 0$, and $d_1 = 0$, $d_2 = 0$ and $d_3 = 1$, which corresponds to

$$H(k) \equiv \begin{pmatrix} 1 & 0 \\ 0 & -1 \end{pmatrix},$$

$$\text{and } P(k) = \frac{1_{2\times 2} - H(k)}{2} \equiv \begin{pmatrix} 0 & 0 \\ 0 & 1 \end{pmatrix}.$$

Less trivial solutions of constraints (36) can be used to construct more interesting projectors. For example, consider the following parameters:

$$c_1 = \frac{1}{3}, \qquad c_2 = \frac{1}{3}\,\mathrm{e}^{\frac{2\pi}{3}\mathrm{i}}, \qquad c_3 = \frac{1}{3}\,\mathrm{e}^{\frac{4\pi}{3}\mathrm{i}}, \qquad d_i = \frac{1}{3}.$$

The corresponding Hamiltonian is given by

$$H(k) = \frac{1}{3}\begin{pmatrix} \left(1 + 2\,\cos\left(k + \frac{4\pi}{3}\right)\right) & (1 + 2\,\cos\,k) - \mathrm{i}\left(1 + 2\,\cos\left(k + \frac{2\pi}{3}\right)\right) \\ (1 + 2\,\cos\,k) + \mathrm{i}\left(1 + 2\,\cos\left(k + \frac{2\pi}{3}\right)\right) & -\left(1 + 2\,\cos\left(k + \frac{4\pi}{3}\right)\right) \end{pmatrix}. \tag{37}$$

The projector $P(k)$ onto the -1 eigenspace can be obtained by using the equation $P(k) = (1_{2\times 2} - H(k))/2$. Since $P(k)$ has matrix elements which are Laurent polynomials in e^{ik}, it is an Strictly local projector.

Having obtained an Strictly local projector, one can use it to construct Hamiltonians which have compactly supported Wannier functions, with any choice of the band energy (flat, or otherwise). For example one may construct a Strictly local flat-band Hamiltonian, with the flat band possessing compactly supported Wannier functions, i.e. orthogonal CLSs. To that end, if $P(k)$ is an Strictly local projector obtained using the method above, we can choose it to correspond to some constant energy, say E. The band associated with the remaining subspace, i.e. the image of $1 - P(k)$, can be chosen to have a dispersion $E(k)$, which should be chosen to be a real function expressible as a Laurent polynomial in e^{ik}. We can also add more bands to our Hamiltonian by constructing another Hermitian matrix $H'(k)$ with entries which are Laurent polynomials in e^{ik}. Arbitrary examples of $H'(k)$ and $E(k)$ satisfying the constraints mentioned above can be easily constructed. Putting it all together, we obtain a Strictly local flat band Hamiltonian $\mathbb{H}(k)$ using

$$\mathbb{H}(k) = H'(k) \oplus [E(k)(1 - P(k)) + EP(k)]. \tag{38}$$

In order to construct an Strictly local flat band Hamiltonian with a larger number of flat bands, one can use the method above to create multiple Strictly local $P(k)$'s and assign a constant energy to each projector. Specifically, we may construct multiple flat band Hamiltonians using (38), and take their direct sum to construct a flat-band Hamiltonian with a larger number of flat bands. Alternatively, one may use the higher dimensional Dirac (or gamma) matrices for an analogous construction. To illustrate the latter procedure, we show how this can be used to construct nearest neighbor projectors on $2d$ lattices in the next subsection.

*A.2.2. 2*d *strictly local projectors.* Similar to the previous subsection, we start with the construction of a flat Hamiltonian H. Here, we choose H to have four bands in order to demonstrate the use of higher dimensional generators of the Clifford algebra. Hence, we express the flat Hamiltonian in terms of Dirac matrices Γ^μ, instead of Pauli matrices, as follows:

$$\begin{aligned}
H(\vec{k}) &= \sum_{\mu=0}^{3} a_\mu(\vec{k})\Gamma^\mu; \\
\text{with } \Gamma^0 = \gamma^0 &= \begin{pmatrix} \mathbb{1}_2 & 0 \\ 0 & -\mathbb{1}_2 \end{pmatrix}, \\
\Gamma^1 = \mathrm{i}\gamma^1 &= \mathrm{i}\begin{pmatrix} 0 & \sigma^x \\ -\sigma^x & 0 \end{pmatrix}, \\
\Gamma^2 = \mathrm{i}\gamma^2 &= \mathrm{i}\begin{pmatrix} 0 & \sigma^y \\ -\sigma^y & 0 \end{pmatrix}, \\
\text{and } \Gamma^3 = \mathrm{i}\gamma^3 &= \mathrm{i}\begin{pmatrix} 0 & \sigma^z \\ -\sigma^z & 0 \end{pmatrix}.
\end{aligned}$$

The Dirac matrices satisfy the anti-commutation relations $\{\Gamma^\mu, \Gamma^\nu\} = 2\delta^{\mu\nu}$ and $\Gamma^{\mu\dagger} = \Gamma^\mu$. For $H(\vec{k})$ to be a nearest neighbor Hamiltonian, the parameters $a_i(\vec{k})$ must be of the form

$$\begin{aligned}
a_i(\vec{k}) = {} & c_{ix}X + c_{ix}^* X^{-1} + c_{iy}Y + c_{iy}^* Y^{-1} + c_{ixy}XY + c_{ixy}^* X^{-1}Y^{-1} \\
& + c_{-ixy}XY^{-1} + c_{-ixy}^* X^{-1}Y + d_i,
\end{aligned} \tag{39}$$

with complex c's, real d's, and $X = e^{ik_x}$, $Y = e^{ik_y}$. $H(\vec{k})^2 = \mathbb{1}$ leads to the condition:

$$\sum_i a_i^2 = 1. \tag{40}$$

Equating the coefficients of all products of all powers of X and Y gives us the following conditions:

$$\begin{aligned}
\sum 2\left(|c_{ix}|^2 + |c_{iy}|^2 + |c_{ixy}|^2 + |c_{-ixy}|^2\right) + d_i^2 &= 1 \\
\sum c_{iy}c_{-ixy} + c_{iy}^* c_{ixy} + c_{ix}d_i &= 0 \\
\sum c_{ix}c_{-ixy}^* + c_{ix}^* c_{ixy} + c_{iy}d_i &= 0 \\
\sum c_{ix}^2 + 2c_{ixy}c_{-ixy} &= 0 \\
\sum c_{iy}^2 + 2c_{ixy}c_{-ixy}^* &= 0 \\
\sum c_{ix}c_{iy} + c_{ixy}d_i &= 0 \\
\sum c_{ix}c_{iy}^* + c_{-ixy}d_i &= 0 \\
\sum c_{ix}c_{ixy} &= 0 \\
\sum c_{ix}c_{-ixy} &= 0 \\
\sum c_{iy}c_{ixy} &= 0 \\
\sum c_{iy}c_{-ixy}^* &= 0 \\
\sum c_{ixy}^2 &= 0 \\
\sum c_{-ixy}^2 &= 0.
\end{aligned}$$

Any solution of these set of equations can used to create a projector. For example, choosing $c_{ixy} = c_{-ixy} = d_i = 0$, the following choice satisfies all the conditions:

μ	0	1	2	3
$c_{\mu x}$	0	0	$\frac{1}{2\sqrt{2}}$	$\frac{i}{2\sqrt{2}}$
$c_{\mu y}$	$\frac{1}{2\sqrt{2}}$	$\frac{i}{2\sqrt{2}}$	0	0

This corresponds to the Hamiltonian:

$$H(\vec{k}) = \frac{1}{2\sqrt{2}} \begin{pmatrix} Y+Y^{-1} & 0 & -(X-X^{-1}) & -(Y-Y^{-1}) + (X+X^{-1}) \\ 0 & Y+Y^{-1} & -(Y-Y^{-1}) - (X+X^{-1}) & (X-X^{-1}) \\ X-X^{-1} & (Y-Y^{-1}) - (X+X^{-1}) & -(Y+Y^{-1}) & 0 \\ (Y-Y^{-1}) & -(X-X^{-1}) & 0 & -(Y+Y^{-1}) \end{pmatrix}.$$

We obtain $P(\vec{k})$ by using $P(\vec{k}) = \frac{1_{4\times4} - H(\vec{k})}{2}$.

ORCID iDs

Pratik Sathe https://orcid.org/0000-0002-9978-8955

References

[1] Wannier G H 1937 The structure of electronic excitation levels in insulating crystals *Phys. Rev.* **52** 191–7
[2] Resta R 2010 Electrical polarization and orbital magnetization: the modern theories *J. Phys.: Condens. Matter* **22** 123201
[3] Thonhauser T, Ceresoli D, Vanderbilt D and Resta R 2005 Orbital magnetization in periodic insulators *Phys. Rev. Lett.* **95** 137205
[4] Arrigo C, Marzari N, Souza I and Nardelli M B 2004 *Ab initio* transport properties of nanostructures from maximally localized wannier functions *Phys. Rev.* B **69** 035108
[5] Ashcroft N W and David Mermin N 1976 *Solid State Physics* (New York: Holt, Rinehart and Winston)
[6] Yates J R, Wang X, Vanderbilt D and Souza I 2007 Spectral and Fermi surface properties from Wannier interpolation *Phys. Rev.* B **75** 195121
[7] Kohn W 1959 Analytic properties of Bloch waves and Wannier functions *Phys. Rev.* **115** 809–21
[8] Cloizeaux J D 1964 Energy bands and projection operators in a crystal: analytic and asymptotic properties *Phys. Rev.* **135** 685A–97
[9] Cloizeaux J D 1964 Analytical properties of *n*-dimensional energy bands and Wannier functions *Phys. Rev.* **135** 698A–707
[10] Nenciu G 1983 Existence of the exponentially localised Wannier functions *Commun. Math. Phys.* **91** 81–5
[11] Marzari N and Vanderbilt D 1997 Maximally localized generalized Wannier functions for composite energy bands *Phys. Rev.* B **56** 12847
[12] Panati G and Pisante A 2013 Bloch bundles, Marzari–Vanderbilt functional and maximally localized Wannier functions *Commun. Math. Phys.* **322** 835–75
[13] Boys S F 1960 Construction of some molecular orbitals to be approximately invariant for changes from one molecule to another *Rev. Mod. Phys.* **32** 296–9
[14] Koster G F 1953 Localized functions in molecules and crystals *Phys. Rev.* **89** 67
[15] Ozolins V, Lai R, Caflisch R and Osher S 2013 Compressed modes for variational problems in mathematics and physics *Proc. Natl Acad. Sci.* **110** 18368–73
[16] Budich J C, Eisert J, Bergholtz E J, Diehl S and Zoller P 2014 Search for localized Wannier functions of topological band structures via compressed sensing *Phys. Rev.* B **90** 115110
[17] Barekat F, Yin K, Caflisch R E, Osher S J, Lai R and Ozolins V 2014 Compressed Wannier modes found from an L_1 regularized energy functional (arXiv:1403.6883)
[18] Zheng L, Liu F and Wu Y-S 2014 Exotic electronic states in the world of flat bands: from theory to material *Chin. Phys.* B **23** 077308
[19] Jerome D and Read N 2015 Tensor network trial states for chiral topological phases in two dimensions and a no-go theorem in any dimension *Phys. Rev.* B **92** 205307
[20] Read N 2017 Compactly supported Wannier functions and algebraic *K*-theory *Phys. Rev.* B **95** 115309
[21] Chen L, Mazaheri T, Seidel A and Tang X 2014 The impossibility of exactly flat non-trivial Chern bands in strictly local periodic tight binding models *J. Phys. A: Math. Theor.* **47** 152001
[22] Leykam D, Andreanov A and Flach S 2018 Artificial flat band systems: from lattice models to experiments *Adv. Phys.:* X **3** 1473052
[23] Yuan C, Valla F, Fang S, Watanabe K, Taniguchi T, Kaxiras E and Jarillo-Herrero P 2018 Unconventional superconductivity in magic-angle graphene superlattices *Nature* **556** 43–50
[24] Yankowitz M, Chen S, Polshyn H, Zhang Y, Watanabe K, Taniguchi T, Graf D, Young A F and Dean C R 2019 Tuning superconductivity in twisted bilayer graphene *Science* **363** 1059–64
[25] Dias R G and Gouveia J D 2015 Origami rules for the construction of localized eigenstates of the Hubbard model in decorated lattices *Sci. Rep.* **5** 16852
[26] Maimaiti W, Andreanov A, Park H C, Gendelman O and Flach S 2017 Compact localized states and flat-band generators in one dimension *Phys. Rev.* B **95** 115135

[27] Maimaiti W, Flach S and Andreanov A 2019 Universal $d = 1$ flat band generator from compact localized states *Phys. Rev.* B **99** 125129
[28] Huber S D and Altman E 2010 Bose condensation in flat bands *Phys. Rev.* B **82** 184502
[29] Kuno Y, Mizoguchi T and Hatsugai Y 2020 Flat band quantum scar *Phys. Rev.* B **102** 241115
[30] Sgiarovello C, Peressi M and Resta R 2001 Electron localization in the insulating state: application to crystalline semiconductors *Phys. Rev.* B **64** 115202
[31] Hejazi K, Chen X and Leon B 2021 Hybrid Wannier Chern bands in magic angle twisted bilayer graphene and the quantized anomalous Hall effect (arXiv:2007.00134 [cond-mat])
[32] Soluyanov A A and Vanderbilt D 2011 Computing topological invariants without inversion symmetry *Phys. Rev.* B **83** 235401
[33] Taherinejad M, Garrity K F and Vanderbilt D 2014 Wannier center sheets in topological insulators *Phys. Rev.* B **89** 115102
[34] Gresch D, Gabriel A, Yazyev O V, Troyer M, Vanderbilt D, Andrei Bernevig B and Soluyanov A A 2017 Z2Pack: numerical implementation of hybrid Wannier centers for identifying topological materials *Phys. Rev.* B **95** 075146
[35] Nakagawa M, Slager R-J, Higashikawa S and Oka T 2020 Wannier representation of Floquet topological states *Phys. Rev.* B **101** 075108
[36] Thouless D J 1984 Wannier functions for magnetic sub-bands *J. Phys. C: Solid State Phys.* **17** L325
[37] Monaco D, Panati G, Pisante A and Teufel S 2018 Optimal decay of Wannier functions in Chern and quantum Hall insulators *Commun. Math. Phys.* **359** 61–100
[38] Panati G 2007 Triviality of Bloch and Bloch–Dirac bundles *Ann. Henri Poincaré* **8** 995–1011
[39] Brouder C, Panati G, Calandra M, Mourougane C and Marzari N 2007 Exponential localization of Wannier functions in insulators *Phys. Rev. Lett.* **98** 046402
[40] Qi X-L 2011 Generic wave-function description of fractional quantum anomalous Hall states and fractional topological insulators *Phys. Rev. Lett.* **107** 126803
[41] Bergman D L, Wu C and Balents L 2008 Band touching from real-space topology in frustrated hopping models *Phys. Rev.* B **78** 125104
[42] Parameswaran S A, Roy R and Sondhi S L 2013 Fractional quantum hall physics in topological flat bands *C. R. Phys.* **14** 816–39
[43] Creutz M 2001 Aspects of chiral symmetry and the lattice *Rev. Mod. Phys.* **73** 119–50
[44] Leykam D, Flach S, Bahat-Treidel O and Desyatnikov A S 2013 Flat band states: disorder and nonlinearity *Phys. Rev.* B **88** 224203
[45] Kuno Y 2020 Extended flat band, entanglement, and topological properties in a Creutz ladder *Phys. Rev.* B **101** 184112
[46] Jünemann J, Piga A, Ran S-J, Lewenstein M, Rizzi M and Bermudez A 2017 Exploring interacting topological insulators with ultracold atoms: the synthetic Creutz–Hubbard model *Phys. Rev.* X **7** 031057
[47] Creutz M 1999 End states, ladder compounds, and domain-wall fermions *Phys. Rev. Lett.* **83** 2636–9
[48] Mukherjee S, Di Liberto M, Öhberg P, Thomson R R and Goldman N 2018 Experimental observation of Aharonov–Bohm cages in photonic lattices *Phys. Rev. Lett.* **121** 075502
[49] Kang J H, Han J H and Shin Y-i 2020 Creutz ladder in a resonantly shaken 1D optical lattice *New J. Phys.* **22** 013023
[50] Löwdin P O 1950 On the non-orthogonality problem connected with the use of atomic wave functions in the theory of molecules and crystals *J. Chem. Phys.* **18** 365–75
[51] Siddharthan R and Antoine G 2001 Square Kagome quantum antiferromagnet and the eight-vertex model *Phys. Rev.* B **65** 014417
[52] Richter J, Derzhko O and Krokhmalskii T 2006 Finite-temperature order-disorder phase transition in a frustrated bilayer quantum Heisenberg antiferromagnet in strong magnetic fields *Phys. Rev.* B **74** 144430
[53] Derzhko O, Richter J and Maksymenko M 2015 Strongly correlated flat-band systems: the route from Heisenberg spins to Hubbard electrons *Int. J. Mod. Phys.* B **29** 1530007
[54] Tasaki H 1992 Ferromagnetism in the Hubbard models with degenerate single-electron ground states *Phys. Rev. Lett.* **69** 1608
[55] Sutherland B 1986 Localization of electronic wave functions due to local topology *Phys. Rev.* B **34** 5208–11
[56] Monaco D and Panati G 2015 Symmetry and localization in periodic crystals: triviality of Bloch bundles with a fermionic time-reversal symmetry *Acta Appl. Math.* **137** 185–203

[57] Brouder C, Panati G, Calandra M, Mourougane C and Marzari N 2007 Exponential localization of Wannier functions in insulators *Phys. Rev. Lett.* **98** 046402
[58] Marcelli G, Moscolari M and Panati G 2020 Localization implies Chern triviality in non-periodic insulators (arXiv:2012.14407)
[59] Yoshioka D 2013 *The Quantum Hall Effect* vol 133 (Berlin: Springer)
[60] Altland A and Zirnbauer M R 1997 Nonstandard symmetry classes in mesoscopic normal-superconducting hybrid structures *Phys. Rev.* B **55** 1142–61
[61] Kitaev A 2009 Periodic table for topological insulators and superconductors *AIP Conf. Proc.* **1134** 22–30
[62] Ryu S, Schnyder A P, Furusaki A and Ludwig A W W 2010 Topological insulators and superconductors: tenfold way and dimensional hierarchy *New J. Phys.* **12** 065010
[63] Katsura H and Koma T 2018 The noncommutative index theorem and the periodic table for disordered topological insulators and superconductors *J. Math. Phys.* **59** 031903
[64] Kitaev A 2006 Anyons in an exactly solved model and beyond *Ann. Phys., NY* **321** 2–111
[65] Marcelli G, Monaco D, Moscolari M and Panati G 2019 The Haldane model and its localization dichotomy (arXiv:1909.03298)